Summer 2022

Synthesis and Characterization of Chitosan Derivatives Intended for Gene Delivery Applications

Alex M. McMullen
Missouri State University, Alex624@live.missouristate.edu

SYNTHESIS AND CHARACTERIZATION OF CHITOSAN DERIVATIVES INTENDED FOR GENE DELIVERY APPLICATIONS

A Master's Thesis

Presented to

The Graduate College of

Missouri State University

In Partial Fulfillment

Of the Requirements for the Degree

Master of Science, Chemistry

By

Alex McMullen

August 2022

SYNTHESIS AND CHARACTERIZATION OF CHITOSAN DERIVATIVES

INTENDED FOR GENE DELIVERY APPLICATIONS

Chemistry

Missouri State University, August 2022

Master of Science

Alex McMullen

ABSTRACT

Chitosan has been studied as a non-viral vector capable of efficient gene delivery due to its favorable properties such as biodegradability, biocompatibility, and is non-toxic to mammalian cells. Incorporating electrostatic interactions in non-viral vectors enhance the vector permeability. This work focuses on two parts. Firstly, cationic chitosan derivatives were synthesized using quarternary ammonium and phosphonium groups. This was achieved by coupling carboxylic acid ligands with these quarternary groups to chitosan through an amide bond. The carboxylic acid ligands were synthesized from 4-methylbenzoic acid and either triethyl phosphine or triethyl amine. The ligand was then attached to chitosan through an amide bond using hydroxybenzotriazole (HOBt) and 1-ethyl-3(3-dimethylaminopropyl)carbodiimide (EDC). These compounds were then analyzed with ^{1}H NMR and FT-IR analyses to determine the extent of incorporation of triethylammonium and triethylphosphonium groups into the chitosan backbone. Electrostatic interactions between these compounds and pDNA were studied using agarose gel electrophoresis. At charge ratios of 4:1 N+:P- or P+:P-both triethyl ammonium and triethyl phosphonium compounds complex with DNA. The second part of the work focuses on previously synthesized derivatives N(1carboxybutyl-4-triethylammonium chloride) chitosan and N(1-carboxybutyl-4-triethylphosphonium chloride) chitosan. These compounds were also studied using dynamic light scattering, zeta potential, and circular dichroism. These compounds were also PEGylated to aid in stability in aqueous media. The size of DNA/polymer complexes were between 140-340 nm at varying concentrations. Zeta potentials showed complete complexation after a weight ratio of 3:1 of polymer to DNA was achieved. Circular dichroism measurements revealed that at weight ratios at 4:1 of polymer to DNA that conformational changes of the DNA would occur. This work aims to investigate the newly synthesized compounds as viable gene therapy candidates capable of enhanced affinity towards nucleotides as well as further studying previously synthesized compounds for their efficiency towards complexing with DNA.

KEYWORDS: chitosan, ammonium, phosphonium, gene therapy, DNA, ^{1}H NMR spectroscopy

SYNTHESIS AND CHARACTERIZATION OF CHITOSAN DERIVATIVES INTENDED FOR GENE DELIVERY APPLICATIONS

By

Alex McMullen

A Master's Thesis
Submitted to the Graduate College
Of Missouri State University
In Partial Fulfillment of the Requirements
For the Degree of Master of Science, Chemistry

August 2022

Approved:

Reza Sedaghat-Herati, Ph.D., Thesis Committee Chair

Richard Biagioni, Ph.D., Committee Member

Gautam Bhattacharyya, Ph.D., Committee Member

Kyoungtae Kim, Ph.D., Committee Member

Julie Masterson, Ph.D., Dean of the Graduate College

ACKNOWLEDGEMENTS

I would like to thank my research advisor, Dr. Herati, for the patience and help he has given me through this process. I would also like to thank my committee members, Dr. Biagioni, Dr. Bhattacharyya, and Dr. Kim for their help in conducting certain experiments and editing the thesis. I would also like to thank Dr. Meints for training me on the NMR instrument and allowing me to use the lyophilizer whenever necessary. Dr. Kim also allowed me to use DNA from his lab, as well as the gel reader used in these experiments, and for that I am grateful. Special thanks to all my colleagues for encouraging me through this process, in particular, Arkanil Roy, Kevin Pinks, Justin Swisher, and Luckio Owoucha. I am very thankful for the moments we shared through our graduate careers. Very special thanks to my wife, Melanie, who has pushed me to become a better writer and scientist.

TABLE OF CONTENTS

LIST OF TABLES

LIST OF FIGURES

CHAPTER 1. INTRODUCTION

1.1. Chitin and Chitosan

Chitin is the second must abundant natural biopolymer behind cellulose. Chitin is a long-chain polymer that consists of *N*-acetylglucosamine. It is found in the cell walls of fungi, exoskeletons of crustaceans and insects, and the scales of fish.[1] Chitosan is the deacetylated form of chitin and is normally prepared by hydrolysis of chitin in aqueous sodium hydroxide.[2] Figure 1 represents the formation of chitosan from chitin using chitin-deacetylase, which is an enzyme that aids in the removal of the acetyl group.[3] The degree of deacetylation can be determined by nuclear magnetic resonance (NMR) spectroscopy. Many of the commercially available chitosans range from 60 to 99% deacetylated. The degree of deacetylation has an impact on the physicochemical and biological properties of chitosan including acid base and electrostatic characteristics, biodegradability, self-aggregation, sorption properties, and the ability to chelate metal ions.[4] Distinguishing between chitin and chitosan is done by looking at the degree of deacetylation where anything 60% or above is considered chitosan.[5] Chitin and chitosan exhibit intramolecular hydrogen bonding through its acetyl and hydroxyl groups giving them three-dimensional α-helices structures.[3,6] The helical structures of chitosan have been studied using solid state X-ray crystallography. However, these helical structures can be changed depending on the experimental conditions such as temperature and pH.[7]

Chitosan structure is closely related to that of cellulose, but it does not share the same properties. Chitosan is insoluble in organic and neutral to basic aqueous solvents. It has been shown that chitin with a degree of deacetylation less than 60% is soluble in dilute acid solutions.[8]

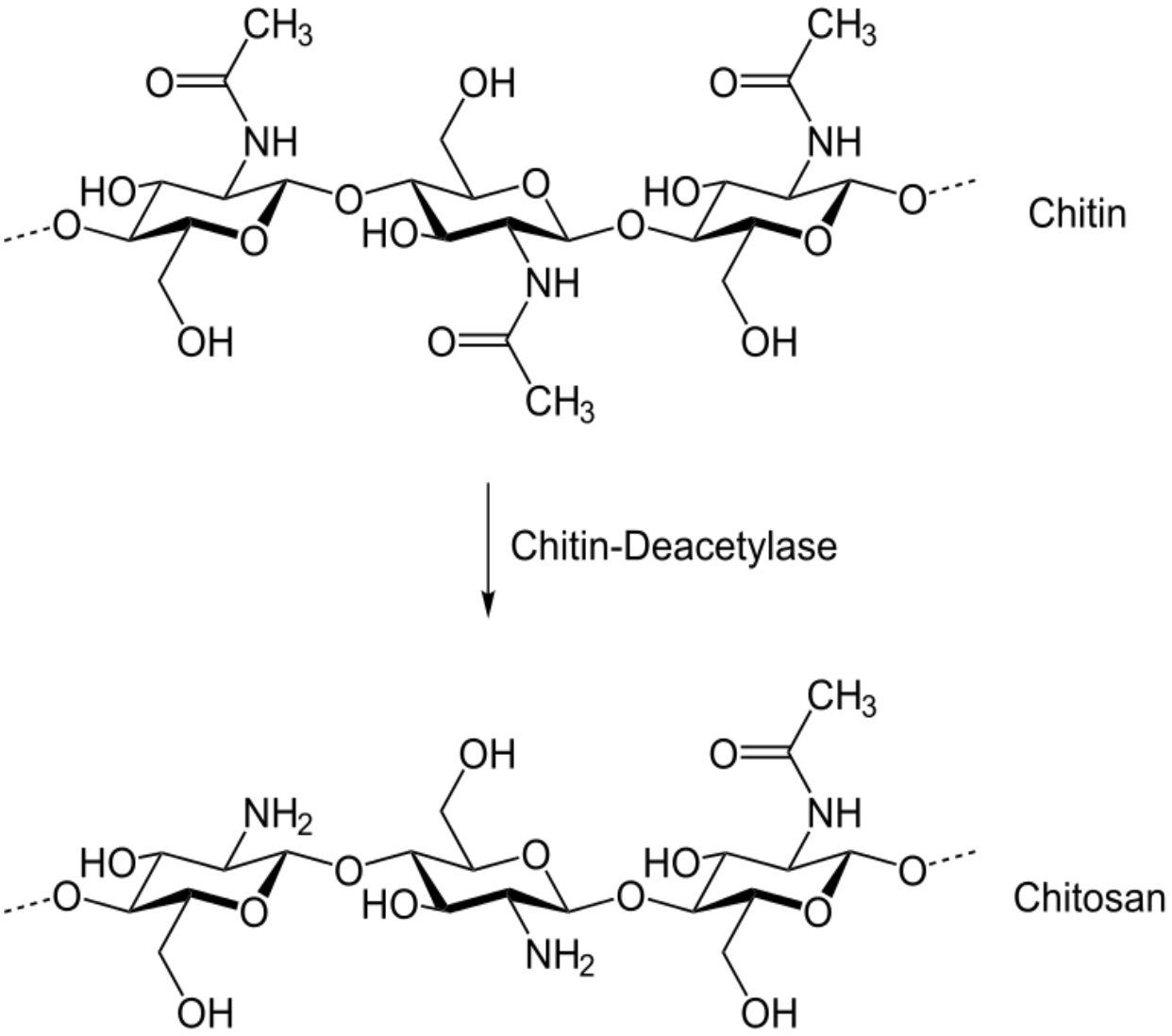

Figure 1. Chitin deacetylation using an enzyme.[3]

At pH 6, the free amino groups found on chitosan's N-deacetylated units begin to protonate, which increases solubility. The increased solubility allows synthetic modifications to take place in solution. The protonation of the amino groups allows for the formation of ionic cross-linking with multivalent anions such as phosphate.[8] Chitosan also has primary and secondary hydroxyl groups that can be synthetically modified once in solution. This ability to alter chitosan's amino and hydroxyl groups allow it to be useful in many applications from soaps, cosmetics, water treatment, protein separation, gene delivery, and cancer treatments.[8,9]

Applications for chitosan are determined by two factors, the degree of deacetylation and its molecular weight (MW). The degree of deacetylation and MW allow for specific physicochemical interactions making chitosan a suitable non-viral vector.[8] The higher the degree of deacetylation, the more amino groups are present for modification and protonation. The stability of chitin's α-helix is disrupted by a higher degree of deacetylation and an increase in protonation of free amino groups. This allows for greater solvation and cationic interactions with chitin. When the degree of deacetylation is lower than 40%, intramolecular hydrogen bonding and hydrophobic methyl groups make chitin insoluble in water.[8,10] When the degree of deacetylation is higher, chitin is less sterically hindered and has less intramolecular interactions making it soluble in aqueous solvents with lower pH.[10–12]

Chitosan microbial degradation is a factor of the degree of deacetylation and distribution of N-acetylated glucosamine units throughout the polymer chain. It was found that once the degree of deacetylation reaches higher than 70% that chitosan's degradation process rapidly declines.[13] Another study showed that chitosan with homogenous distribution of N-acetylated glucosamine units was less susceptible to degradation within lysosomal space.[14] With the

control of these two parameters, chitosan's ability to degrade within biological systems can be affected.

MW can significantly affect chitosan's function in a variety of applications that include burn healing, coagulation of pollutants, lowering blood cholesterol levels, enhancing drug dissolution, control of viscosity, and improving crop yields.[8,15] Different MW have been shown to influence the growth of *E. coli.* cells. Higher MW prevented *E. coli.* growth, while lowering the MW promoted it. Sodium nitrite can be used to depolymerize chitosan controllably, allowing for a wide range of MW chitosan.[16] The MW can also determine the strength of interaction between DNA and chitosan. In acidic solution, electrostatic attraction between protonated chitosan and DNA occurs. Higher MW chitosan can wrap around short (24 base pair) double-stranded DNA and create a stronger interaction through entanglement.[17] Because low MW chitosan does not exhibit this entanglement effect, it is less effective at condensing short double-stranded DNA.[18] The electrostatic attraction between DNA and chitosan is generated by the protonation of the free amino groups on chitosan. When the pH is increased, the interaction is lost as a result of the deprotonating of the amino groups.

Chitosan can be chemically modified to bear pH-independent cationic groups that can provide sustained interactions with short double-stranded DNA through a broad pH range.[16] The degree of complexation of short double-stranded DNA with chitosan can be controlled by changing the positive to negative charge ratio (+/-).This ratio is determined by the amount of negatively charged phosphate groups on DNA and comparing that to the positively charged ammonium or phospohonium groups on chitosan. Many advantages are associated with using cationic macromolecules to bind DNA including ease of functionalization, higher stability relative to lipoplexes, and lower toxicity.[19] Chitosan derivatives have also shown to bind to

specific moiety that viral vectors cannot.[20] Synthesizing chitosan derivatives with cationic functional groups that are not dependent on pH can provide a way for chitosan to become a viable non-viral vector suitable for gene therapy.

1.2. Chitosan Modification

Modifications have been made to chitosan to improve solubility in neutral conditions. Chitosan derivatives with various functional groups have been prepared for various applications in the biomedical field as seen in Figure 2.[21] Chitosan's amino and primary hydroxyl groups allow for chemical modification that can lead to an increase in solubility and affinity for nucleotides. Hydroxyl groups can be modified to carboxymethyl groups in order to increase solubility. Chitosan itself is non-toxic to mammalian cells, but the addition of cationic groups can increase toxicity.[22]

One such modification requires coupling carboxylic acids to amino groups to form a more stabilized amide. This coupling requires a preliminary activation step to create a stable intermediate that is more reactive toward amino groups.[23] In 1995, experiments were conducted to observe the effects on coupling efficiency using altered carbodiimides.[24] N,N'-dicyclohexylcarbodiimide (DCC) and 1-ethyl-3-(3-dimethylaminopropyl)carbodiimide (EDC) were reacted with various nucleophiles to observe the reaction mechanism. For both EDC and DCC, the rate-limiting step was the formation of O-acylisourea, where the fully-protonated carbodiimide and the carboxylate ligand react to form a reactive intermediate. The O-acylisourea complex is very reactive and short-lived in solution.[23] At a pH lower than six, the intermediate hydrolizes, thus reforming the carboxylic acid ligand and a deactivated EDC-urea. At pH's between 6-8, the intermediate remains in solution long enough to encounter amino

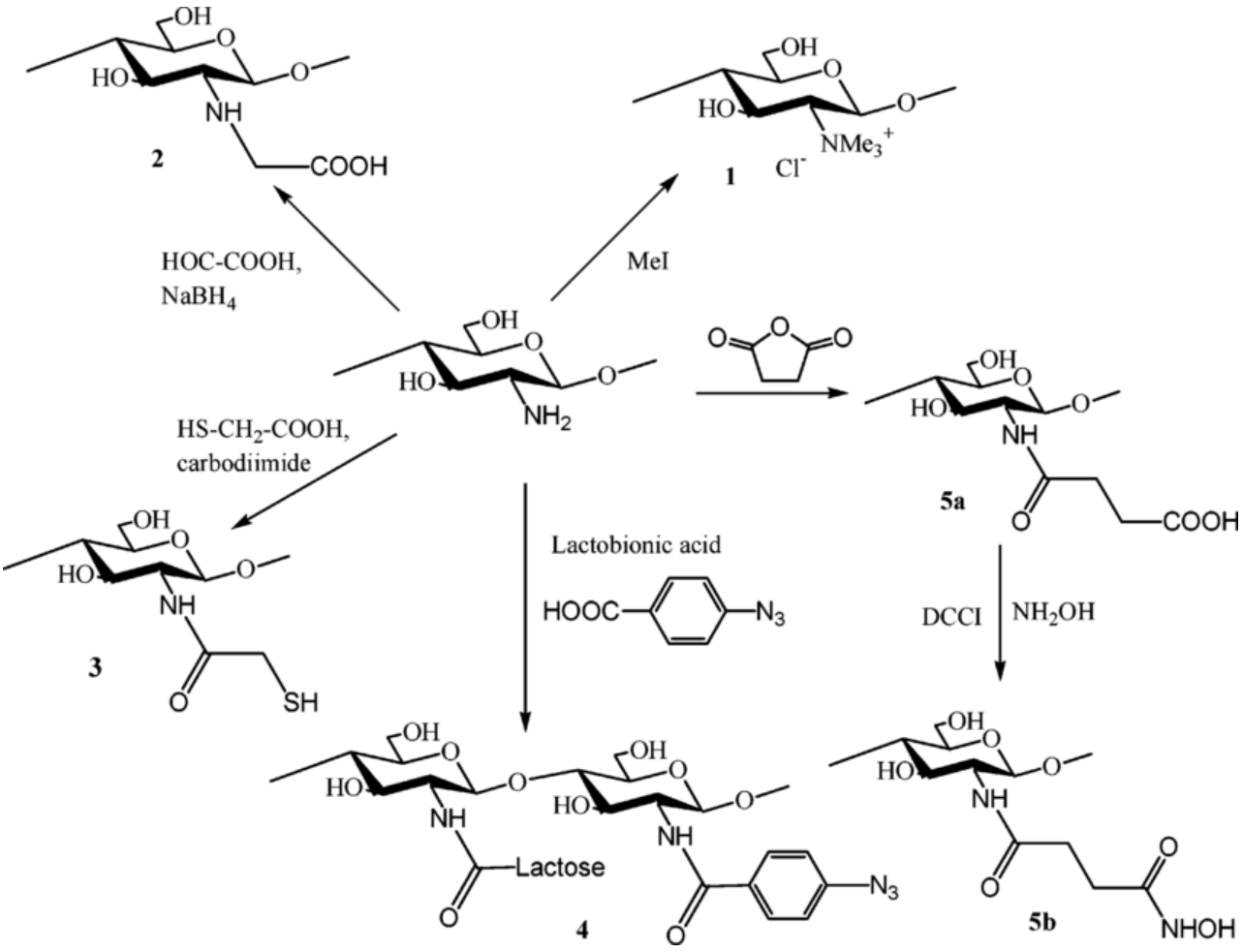

Figure 2. Examples of chitosan derivatives for biomedical applications.[21]

groups and undergo successful coupling. Using EDC and DCC has been shown to be successful when coupling carboxylic acids to amino groups, but other additives have been studied to improve coupling efficiency. Hydroxybenzotriazole (HOBt) has been used in carbodiimide reaction schemes to stabilize the O-acylisourea intermediate. HOBt attacks the activated EDC-carboxy intermediate and forms a more stable intermediate that can remain in solution for an extended period of time, increasing the overall efficiency of the EDC/HOBt coupling scheme.[23] The primary amines on chitosan can be linked with functionalized carboxylic acids using EDC and HOBt.[22,25] Water-soluble EDC can be used to make these modifications at room temperature under open air conditions. Cationic modification to chitosan is done by first using EDC followed by HOBt. These modifications allow chitosan to interact with short double-stranded DNA.[24,26] Figure 3 illustrates the mechanism for these carboxylic acid attachments to chitosan.[27]

1.3. PEGylation

PEGylation is defined as the coupling of polyethylene glycol (PEG) to other materials. Chitosan's ability to interact with DNA has been improved through several modifications including PEGylation.[26] The Food and Drug Administration (FDA) has approved of the use of PEG in biomedical and biotechnical fields. It has been used in many applications from cosmetics to drug delivery systems.[28] PEGs are classified as polyethers, linear and branched, that have molecular weights ranging from 300 to 40,000 g/mol.[28] PEGs with lower molecular weights have lower melting points and are liquids at room temperature. High molecular weight

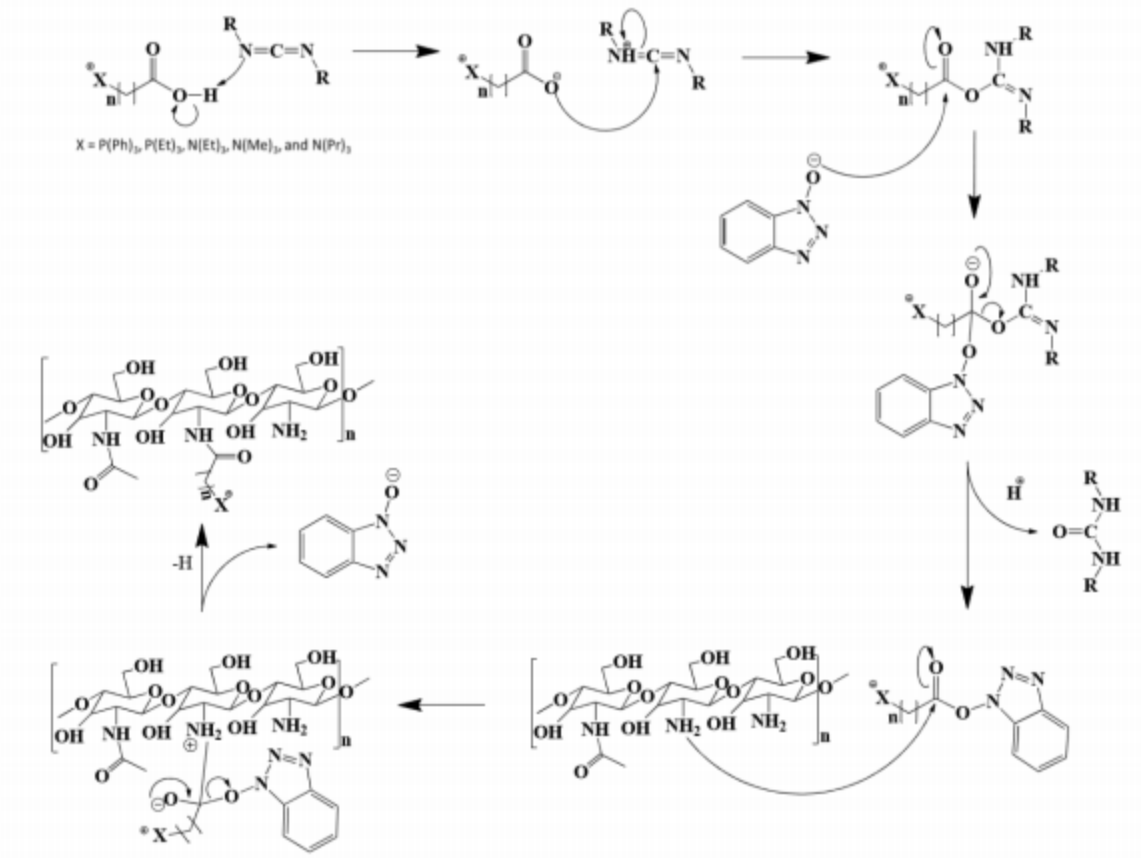

Figure 3. Reaction Mechanism of EDC and HOBt coupling carboxylic acid ligand to chitosan.[27]

PEGs have higher melting points and are crystalline at room temperature. These behaviors can be explained by looking at chain length. The high molecular weight PEGs have longer chains. These longer chains become entangled and create more intermolecular forces that increase the melting point.[29] The most commonly used PEG is methoxy polyethylene glycol (mPEG). This derivative contains a hydroxyl group at one end and a methoxy group at the other.[28] PEGs are soluble in many aqueous and organic solvents making them a prime candidate for work with organic transformations. Adding PEGs to medications and gene delivery vectors increases solubility which then increases the medications efficiency.[28] PEGylating chitosan produces

conjugates with reduced toxicity and increased stability in aqueous media.[28] Introducing PEG into pharmaceutical applications, such as gene therapy, is often encouraged.[30] PEG-grafted chitosan has been prepared to lower toxicity of certain cationic chitosan derivatives and increase water solubility.[28] These PEG-grafted non-viral vectors have been shown to stabilize complexation of short double-stranded DNA through shielding of the positive charges present on modified vectors. PEG-grafted vectors have displayed higher solubility and complexation with short double-stranded DNA when compared to their non-PEGylated counterparts.[30]

1.4. Gene Therapy

Chitin and chitosan have been studied for their application in gene therapy since the early 1990's when their structures were identified using infrared spectroscopy (IR). Chitosan compounds are among the non-viral vectors heavily researched for gene delivery due to their low toxicity in mammalian cells and naturally high abundance.[8] Therapeutic fields have been researching gene therapy for over twenty years.[25] Introduction of new genetic material to diseased genes has been shown to restore functionality of damaged genes.[31] This same method has also been used to investigate inherited single gene disorders.[31] Gene delivery vectors, or vehicles, are needed to transfer new genetic material into or near the desired therapeutic sites. The transfer of this material can occur through techniques such as *ex vivo, in vivo,* or *in situ.*[8]

Viral and non-viral vectors are utilized with many gene therapy approaches.[3] Viral gene delivery uses viruses to infect cells with the new genetic material. These viruses can be modified to stop their reproductive cycle by removing genetic sequences needed for reproduction. However, they require sequencing of the viruses for binding and gene delivery to be useful.[32] Commonly used viral vectors include retrovirus,[8,33,34] adenovirus,[8,9] adeno-

associated viruses,[35] herpes virus,[36] and vaccinia virus.[8,37] Each of the listed viral vectors has been incorporated into its own unique application. A few of these viruses can produce sustained gene expression but only in cells that divide. Others are just as effective against non-dividing cells without integrating into their host cell chromosome.[38] Viral DNA can integrate into the genomes of the cell causing mutations in the cell that lead to safety concerns.[32] The safety concerns of viral gene delivery began to grow after the accidental death of a patient using gene therapy for immune deficiency.[22] Due to the fear of using viral vectors, increased investigations into using non-viral vectors have been pursued.

Non-viral vectors can deliver large fragments of genetic material to mammalian cells comparable to that of viral vectors.[22] These vectors have been successful, but are less effective than viral vectors in transfecting mammalian cells.[39] There have been many investigations for improving these non-viral vectors for gene delivery. Addition of cationic polymers, mainly dendrimers and short chain oligomers, have been found to meet the pharmaceutical standards for human use.[40] Dendrimers have been shown to form complexes with plasmid DNA (pDNA) and are regarded as one of the most effective non-viral vectors.[41] However, there have been recent studies that have raised concern over the use of dendrimers in biological systems due to their toxicity.[42,43] Decreasing the molecular weight and lowering the degree of branching of these dendrimers have been shown to slightly lower the toxicity in biological systems.[44–46] Cationic polymers that can be formed in long-chain fashion or polycationic-spherical balls have been shown to have increased interaction with pDNA.[44–47] Short-chain polymers have been shown to have weaker interactions and lower overall solubility.[42,43] Linear polysaccharides, such as chitosan, have been proposed as biocompatible gene delivery vectors that can be tailored for electrostatic interactions. Studies have shown that chitosan exhibits low cytotoxicity within

mammalian cells and displays viability in gene therapy.[44–48] Current research shows that high molecular weight chitosan derivatives have been shown to exhibit the highest complexation and stability with pDNA.[31,49–52]

1.5. Particle Sizing and Zeta Potential

When the chitosan compound complexes with DNA, the complex must meet a certain size requirement before uptake in the cells will happen. Particles with diameters less than 0.5 μm are internalized through phagocytosis while particles with diameters less than 0.2 μm are internalized through pinocytosis.[53] In a study done by Kim et al., most of the modified chitosan/DNA complex nanoparticles were below 400 nm in diameter.[54] These diameters are normally determined by dynamic light scattering (DLS). This technique utilizes light rays and how they scatter when they hit small particles. When the light scatters, its intensity fluctuates due to the particles' Brownian motion. The scattered light also interferes, either constructively or destructively, with other particles in the solution. Depending on how the scattered light interacts with the particles, size can be determined by the Stokes-Einstein equation. This equation provides the hydrodynamic radius of the particles which is used in most studies.[55]

Another useful tool for determining complexation with DNA is zeta potential. The zeta potential is the electrical potential at the slipping plane. This plane is the interface which separates mobile fluid from fluid that remains attached to the surface. Zeta potential is caused by the net electrical charge contained within the region bounded by the slipping plane. For this reason, it is used for quantification of the magnitude of the charge of the fluid.[56] It is determined through electrophoresis, meaning that an electric field is applied to the solution. Particles with a zeta potential will migrate to the electrode of opposite charge with a velocity proportional to the

zeta potential. A laser is used to determine the velocity. As the particles move to the electrode, they shift the frequency of the laser. This shift is then converted to the particle mobility which is then converted to zeta potential by inputting the viscosity and dielectric permittivity and applying the Smoluchowski theories.[57] When the zeta potential is negative, the net charge of the particles is negative. When it is positive, the overall charge of the particles is positive. Since DNA has phosphate groups on the backbone, particles in the solution containing only DNA will be negatively charged. Chitosan compounds used for vectors are positively charged, so the particles in a solution of modified chitosan compounds will have a positive zeta potential. Complexation can be determined by measuring naked DNA and adding increasing amounts of chitosan compounds. As the chitosan complexes with DNA, the zeta potential will become less negative. Once complete complexation has occurred, the zeta potential will be zero. Adding more chitosan compounds past this point will result in a solution with positive charge. In this work, the zeta potential was used alongside gel electrophoresis to determine complexation.

1.6. Previous Work

Previous studies have shown that adding ammonium, phosphonium, and mPEG groups to chitosan increases solubility and electrostatic interactions with DNA. Multiple groups have added phosphonium groups to chitosan for non-viral gene vectors using HOBt, and EDC. They found that the derivatives were soluble in aqueous solutions and had very low toxicity.[31,58,59] Using this information, we decided that adding these groups onto chitosan would be beneficial. In previous studies, Wyatt synthesized two different compounds containing the ammonium and phosphonium groups, N-(1-carboxybutyl-4-triethylammonium chloride) chitosan (TEAB-CS) and N-(1-carboxybutyl-4-triethylphosphonium chloride) chitosan (TEPB-CS). The procedure

for synthesizing these compounds used hydroxybenzotriazole (HOBt) and 1-ethyl-3-(3-dimethylaminopropyl) carbodiimide (EDC) as the coupling agents for the coupling of the amines or phosphines to carboxylic acids. Once the carboxylic acid and amine/phosphine are coupled, the carboxylic acid can react with an amine on chitosan to form an amide bond. The resulting compounds could then be analyzed using proton nuclear magnetic resonance (^{1}H NMR) to determine the percent substitution of the amine/phosphine group on chitosan.[27] These compounds showed increased solubility as well as electrostatic interaction with DNA. However, size of the complexes were never studied, an important factor in the process of cellular uptake.

Other groups such as Kean et al. have synthesized trimethylated chitosan derivatives for use in non-viral gene delivery. This process involved dissolving chitosan in 1-methyl-2-pyrrolidinone (NMP) with sodium iodide. Sodium hydroxide was then added to maintain an alkaline environment. Methyl iodide was added to the solution in order for methylation to occur through nucleophilic substitution. The derivatives cytotoxicity's were then studied to determine viability as a gene delivery vector. It was found that these compounds are less toxic than the gold standard of linear polethylenimine. These compounds also interacted with pDNA at weight ratios of 10:1 (w/w derivative:pDNA) when studied using agarose gel electrophoresis. [60] These studies serve as the basis of the work presented in this thesis.

1.7. Purpose of this Work

In this research, two goals were established. Firstly, synthesis of ammonium and phosphonium chitosan derivatives different than those prepared by Quinton Wyatt. Wyatt synthesized chitosan derivatives that had short alkyl chains attached to a triethylammonium or triethylphosphonium group. The compounds that were synthesized in this work have a benzene

ring between the ammonium/phosphonium group and the amide bond on chitosan. These compounds aim to increase the hydrophobicity while still providing the same amount of electrostatic interaction with DNA. Using previous established methods for synthesizing chitosan derivatives, two novel compounds were synthesized, N-(1-carboxymethyl-4-triethylammonium chloride) methylbenzoic acid (TEABA-CS) and N-(1-carboxymethyl-4-triethylphosphonium chloride) methylbenzoic acid (TEPBA-CS). Triethyl ammonium/phosphonium benzoic acid ligands were attached to 95% DA chitosan using HOBt and EDC. To determine if the degree of substitution could be manipulated, differing amounts of ligand were attached to the same amount of chitosan in multiple reactions. These cationic chitosan derivatives were then analyzed using ^{1}H NMR and Fourier Transform-Infrared Spectroscopy (FT-IR) to prove that the ligand had attached to chitosan. Agarose gel electrophoresis was then used to determine concentrations at which complexation with DNA occurs. The second goal of this work was to complete characterization of Wyatt's compounds (TEAB-CS and TEPB-CS). The compounds were first PEGylated and studied using gel electrophoresis. Circular Dichroism (CD) was used to study the effect of these compounds on DNA conformation. Size, zeta potential, and solubility studies were conducted to finish the work on these compounds. Figure 4 shows the chitosan derivatives worked on for this project.

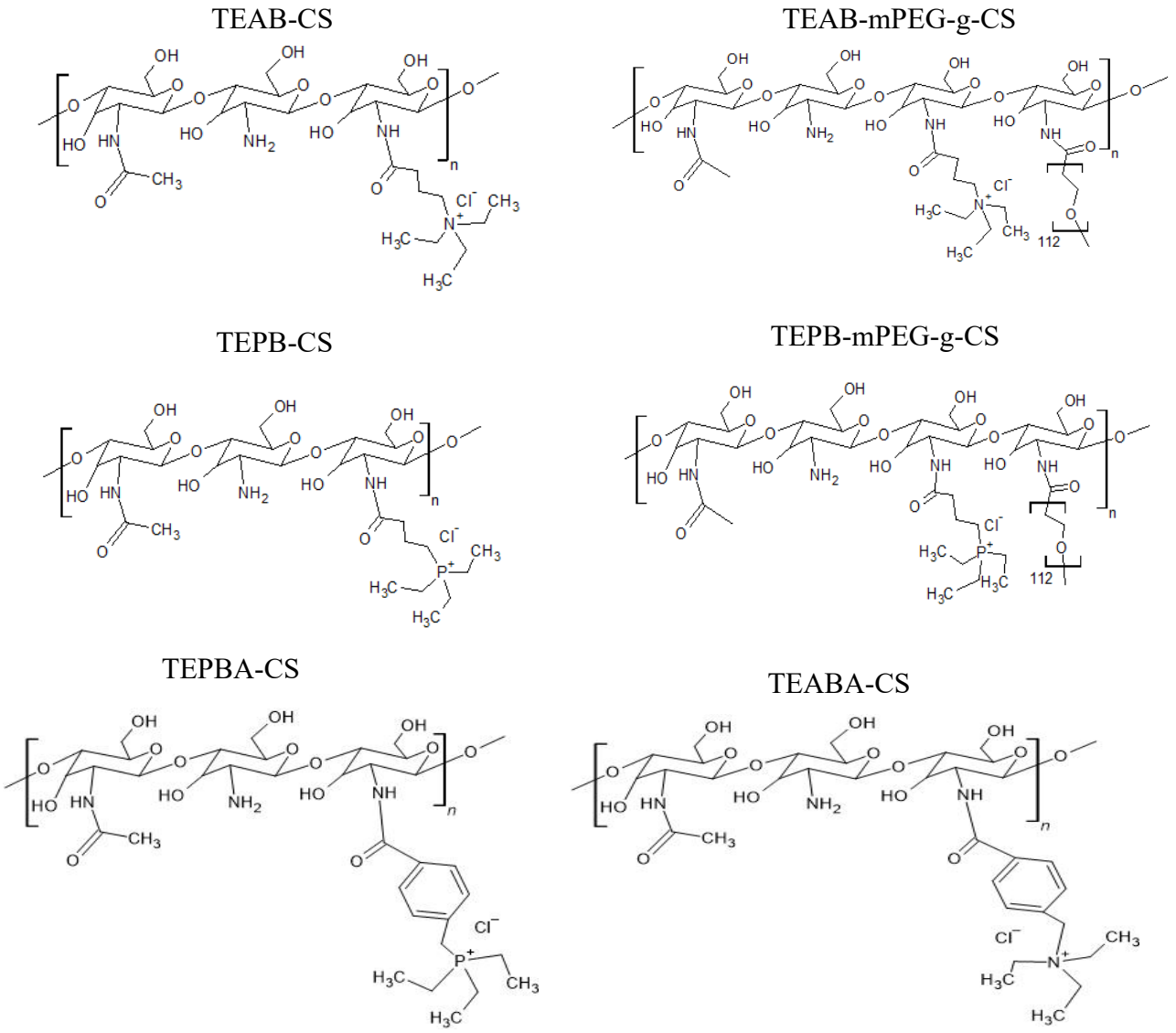

Figure 4. Chitosan derivatives prepared and used in this study.

CHAPTER 2. EXPERIMENTAL METHODS

2.1 Materials and Instrumentation

2.1.1 Materials. 95% deacetylated chitosan (medical grade) was purchased from Bonding Chemical Co.. 4-(bromomethyl) benzoic acid, methyl-4-(bromomethyl) benzoate, triethyl amine, triethyl phosphine, calf thymus DNA, and ethyl alcohol were purchased from Sigma Aldrich. 1-Ethyl-3-(3dimethylaminopropyl) carbodiimide (EDC) was purchased from Chem Empex. DMSO, DMSO-d_6, D_2O, and hydroxybenzotriazole (HOBt) were purchased from Alfa Aesar. Dr. Kyoungtae Kim provided the pDNA used for the gel electrophoresis.

2.1.2. Nuclear Magnetic Resonance (NMR). The carboxylic acid ligands and chitosan derivatives were studied using ^1H NMR spectroscopy on a Varian 400 MHz NMR spectrometer. Bruker TopSpin processor software was used for data analysis of the spectra. Studies were conducted at 25°C in D_2O or DMSO. D_2O was used for the chitosan derivatives and DMSO was used for the carboxylic acid ligands. Samples were prepared by weighing out 2 mg of compound and placing in 700 μL of solvent. These samples were then placed in a Branson 2510 ultrasonic bath for 15 minutes to completely dissolve. The samples were analyzed using 5 second acquisition time, 5 second relaxation, 90º pulse angle, and auto gain control. The results for these studies are found in Appendix A.

2.1.3. Fourier-Transform Infrared Spectroscopy (FT-IR). The synthesized compounds were studied using Fourier-transform infrared spectroscopy to confirm the coupling of the carboxylic acid ligands to N-glucosamine units. A Bruker Vertex 70 FT-IR with Bruker OPUS 7.5. software was used for these analyses. Experiments were conducted using KBr pellets. Briefly, 1 mg of sample was added to 100 mg of KBr. All runs were carried out using a

wavenumber range of 4000-400 cm^{-1}, 2 cm^{-1} resolution, 100 scans, and automatic atmospheric correction. The results for these studies are found in Appendix B.

2.1.4. Agarose Gel Electrophoresis. Agarose gel electrophoresis was conducted in pH 7.4 tris acetate EDTG (TAE) buffer using 2% agarose gels, 2 µL of pDNA (187 µg/mL), 2 µL of loading dye, and varying amounts of chitosan derivatives to give N^+/P^- or P^+/P^- ratios from 8 to ½ (where P^- is the phosphate on DNA and N^+ or P^+ is the ammonium or phosphonium group on chitosan). Visualization was done using an Azure biosystems gel reader.

2.1.5. Circular Dichroism (CD). CD analysis was conducted using a Jasco J-815 spectrometer coupled with a PFD-425s single positions peltier. Samples were loaded into a cuvette with a path length of 1 mm and volume of 400 µL. Distilled deionized water was used for background measurements. After background measurements, calf thymus DNA was added to the cuvette to a final concentration of 100 µg/mL and scanned. After this scan, increasing amounts of chitosan derivatives were added to the DNA solution to give weight ratios from 1 to 16. Each sample was scanned 3 times at a speed of 50 nm/min at room temperature. Data points were collected every 0.025 nm. The results were then exported to Microsoft Excel and processed. Results from these studies are found in the Results and Discussion Section.

2.1.6. Dynamic Light Scattering (DLS) Size Determination. Particle size for the polymer/DNA complexes at various weight ratios were determined using Brookhaven NanoBrook Omni particle analyzer with BIC operating software. Samples were prepared in both water and PBS buffer (7.4) to a final volume of 3 mL. Calf DNA was added to a final concentration of 100 ug/mL. Chitosan compounds (1mg/mL) were then added in weight ratios from 1 to 10 then allowed to sit for 15 minutes. Measurements were taken at a 90º

backscattering angle for 90 seconds and run in triplicate. Results are discussed in the Results and Discussion section.

2.1.7. Zeta Potential. Zeta potential studies were done with polymer/DNA complexes similar to those for DLS size measurements. The Brookhaven NanoBrook Omni particle analyzer was used with BIC operating software. An electrode provided by Dr. Adam Wanekaya was used to deliver the voltage in the sample. Samples were prepared in water to a final volume of 1.5 mL. Calf DNA was added to a final concentration of 15 μg/mL. Chitosan derivatives (1mg/mL) were then added in weight ratios from 1:8. Measurements were taken using 3 cycles of electric charge passing through the solution. After 3 cycles, the zeta potential was averaged by the instrument. Each sample was run in triplicate and results are discussed in the Results and Discussion section.

2.1.8. Solubility Studies. Solubility studies were conducted using a Varian Cary 50 UV-Vis spectrophotometer. 1.00 mg of chitosan and its derivatives were dissolved in 5.00 mL of 1% aqueous acetic acid. The pH was gradually increased using 0.1 M NaOH until a pH of 10 was obtained. %T data was collected at various pH ranges from 1.75 to 10. A Fisher Science 810 series pH meter was used to determine pH. The wavelength of 600 nm was used in %T evaluation. The compounds do not absorb at this wavelength, but when a phase separation occurs, such as that when the compounds become insoluble, then the light scattering is significant and used to determine solubility points.

2.2. Synthesis of Methyl-4-(triethylammonium bromide) Methyl Benzoic Acid

2.000 g of methyl-4-(bromomethyl) benzoate was placed in 2.5 mL of triethyl amine. The contents were placed in 50 mL of methanol and refluxed overnight. Methanol was evaporated using a Heidolph model 036000820 rotary evaporator. An oily substance was formed

and completely dried using a vacuum oven. After drying, the compound was hydrolyzed using 3M HCl and refluxed overnight. The mixture was allowed to cool and solvent was evaporated using a Heidolph model 036000820 rotary evaporator. This resulted in an oily substance that was washed and precipitated with cold acetone. After the washing with 10 mL acetone, the precipitate was collected and dried in a vacuum oven for 2 days. This yielded 2.881 g of product (75% yield). The final product was examined using ^{1}H NMR spectroscopy for full reaction. The reaction scheme for the synthesis of ethyl-4-(triethylammonium bromide) methyl benzoic acid (TEABA) is detailed in Figure 5.

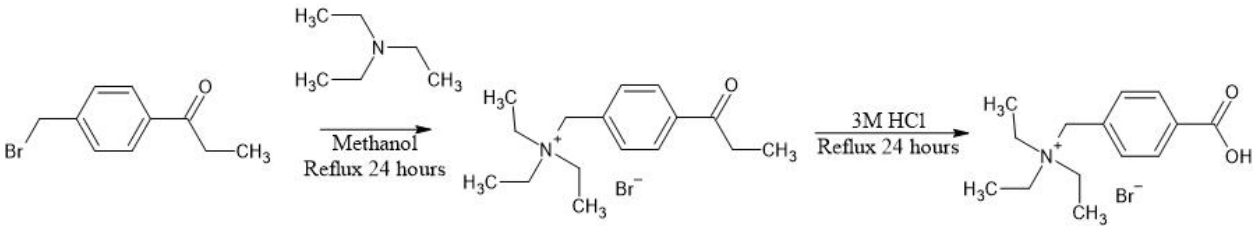

Figure 5. Reaction scheme for synthesis of TEABA ligands.

2.3. Synthesis of Methyl-4-(triethlyphosphonium bromide) Methyl Benzoic Acid

4.000 g of 4-Bromomethyl benzoic acid was placed in 150 mL of toluene. Under an atmosphere of nitrogen, 2.8 mL of triethyl phosphine was added to the mixture and refluxed for 24 hours. A white precipitate formed and was filtered out of solution then washed with diethyl ether 3 times. The washed precipitate was dried in a vacuum oven overnight. The final product was methyl-4-(triethlyphosphonium bromide) methyl benzoic acid (TEPBA) and yielded 5.624g (90% yield). Figure 6 shows the reaction scheme for the phosphonium carboxylic acid ligand.

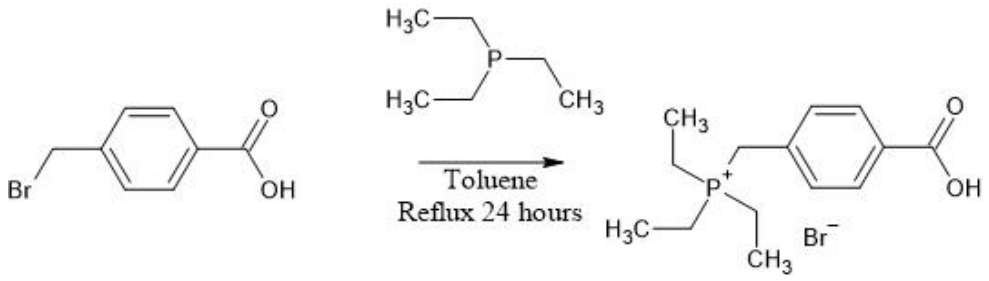

Figure 6. Reaction scheme for synthesis of TEPBA ligands.

2.4. Synthesis of Ammonium/Phosphonium Chitosan Derivatives

Mole ratios of chitosan to carboxylic acid derivatives were calculated to help determine if the degree of substitution of ligand could be controlled. Ratios used were from 1:1 (acid:chitosan) to 5:1. The corresponding amount of acid ligand was then dissolved in 2 mL of DMSO. In another solution, 0.250 g of 95% deacetylated chitosan were suspended in 20 mL of water. 0.750 g of HOBt were dissolved in 10 mL of DMSO and added dropwise to the chitosan solution. This was allowed to stir until completely soluble. Once soluble, the acid ligand solution could be added along with 0.850 g of EDC. This mixture was stirred for 24 hours. After stirring, the solution was dialyzed using a molecular weight cutoff 12,000 KDa cellulose dialysis tube suspended in deionized water. The water was dumped and replaced every 24 hours and the tube was in water for 3 days. The solution within the tube was then frozen using liquid nitrogen and lyophilized for 3 days. The freeze dried product was analyzed using ^{1}H NMR spectroscopy to determine reaction completion and degree of substitution. The final products were the ammonium/phosphonium carboxylic acid substituted chitosan derivatives. Varying reactions were conducted with yields from 26-88 %. Figure 7 shows the scheme for this reaction.

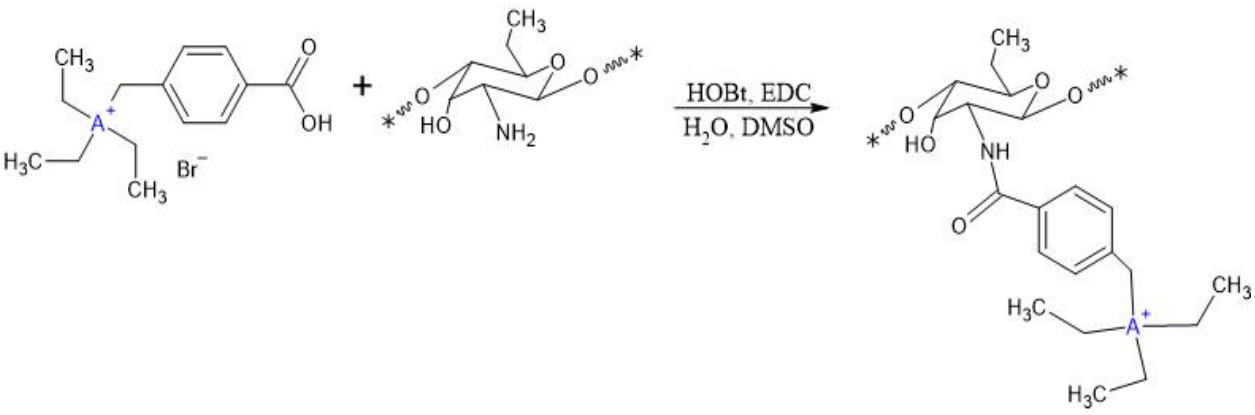

Figure 7. Reaction scheme for attaching carboxylic acid ligands to chitosan. A^+ represents either N^+ or P^+.

2.5. PEGylation of TEAB-CS and TEPB-CS

TEAB-CS was PEGylated by dissolving 0.60 g of the compound in 22.5 mL of 2:1 (v:v) H_2O/DMSO mixture. 0.13 g of HOBt, 0.18 g of EDC, and 1.00 g of mPEG (5000) acetic acid were added to the solution and stirred overnight. Another portion of 0.13 g of EDC were added and stirred for an additional 4 hours. The mixture was dialyzed for two days and then freeze-dried. The product was soaked in methylene chloride and filtered and washed 3 times, each time with 5 mL of fresh methylene chloride and then dried to obtain 0.43 g of the product.

TEPB-CS PEGylation was carried out the same way as TEAB-CS-g-mPEG. 0.40 g TEPB-CS, 0.13 g HOBt, 1.03 g mPEG (5000) acetic acid, and 0.18 g EDC yielded 0.60 g of product. The DS for grafting mPEG into chitosan was determined by ^{1}H NMR for both compounds and is discussed in the Results and Discussion section.

CHAPTER 3. RESULTS AND DISCUSSIONS

3.1 ^{1}H NMR Analysis

3.1.1. Ammonium and Phosphonium Carboxylic Acid Ligands. The carboxylic acid ligands containing ammonium and phosphonium groups were analyzed with ^{1}H NMR spectroscopy. These compounds were 4-methyltriethylammonium benzoic acid and 4-methyltriethlyphosphonium benzoic acid. The results of each study can be viewed in Appendix A. Integration lines and their values are indicated in red. Peak signals are labeled with numbers above the spectra corresponding to the chemical shift of that peak. After drying of the samples, 2 mg of each were dissolved in 700 µL of DMSO or D_2O. Chemical shift values for both ammonium and phosphonium carboxylic acid ligands are shown in Table 1.

Table 1. ^{1}H NMR assignments for synthesized carboxylic acid ligands

Ligand Name	Abbreviation	^{1}H NMR ppm
methyl-4-(triethlyammonium bromide) methyl benzoic acid	TEABA	7.95, 7.50 (4H, -$C_6\mathbf{H_6}CH_2N^+(CH_2CH_3)_3$), 4.34 (2H, -$C\mathbf{H_2}N^+(CH_2CH_3)_3$), 3.11 (6H, -$N^+(C\mathbf{H_2}CH_3)_3$), 1.25 (9H, -$N^+(CH_2C\mathbf{H_3})_3$)
methyl-4-(triethlyphosphonium bromide) methyl benzoic acid	TEPBA	7.89, 7.31 (4H, -$C_6\mathbf{H_6}CH_2P^+(CH_2CH_3)_3$), 3.64 (2H, -$C\mathbf{H_2}P^+(CH_2CH_3)_3$), 2.05 (6H, -$P^+(C\mathbf{H_2}CH_3)_3$), 1.05 (9H, -$P^+(CH_2C\mathbf{H_3})_3$)

Both spectra show two peaks from 7.30 ppm and 7.95 ppm (2H) which are assigned to the protons on the benzene ring. TEPBA shows peaks with heavy splitting at 1.05 ppm (9H)

corresponding to the end methyl groups on the phosphonium group. The integration for the benzene hydrogens were 1.00 and 1.09, indicating that integration was done properly. This would mean that each hydrogen has an integration value of 0.53 after averaging the two integrals. The integrals from the heavily split peak at 1.05 ppm has an integral value of 4.85. This means that each hydrogen was integrated with a value of 0.54. These numbers match up relatively well and show that successful substitution of bromide for triethylphosphine had occurred. In TEABA spectrum, the benzene peaks have integrations of 1.00 and 1.09 giving a single hydrogen integration value of 0.53. The peak from the end methyl groups at 1.25 ppm have an integration of 5.06 which results in each hydrogen having an integral value of 0.56. These numbers are consistent and again show complete substitution of bromine with triethylamine.

An interesting difference in the two spectra show that the peaks assigned to the same hydrogens ($X^{+}(C\mathbf{H_2}CH_3)_3$) have shifted quite substantially. In TEPBA, the peak is labeled at 2.05 ppm while for TEABA that same peak is at 3.11 ppm. This can be attributed to the shielding effect caused by the difference of phosphorus and nitrogen. Since nitrogen is more electronegative, the deshielding from it is greater and causes a large shift downfield. This can be seen in the spectra in Figure 8.

3.1.2. Ammonium and Phosphonium Chitosan Derivatives. Chitosan derivative prepared from the quarternary carboxylic acid ligands were also studied using ^{1}H NMR. Again, these spectra can be found in Appendix A. Each sample was prepared using 2 mg of the polymer and 700 μL of D_2O. Then it was placed in the ultrasonic bath to completely dissolve. Red lines indicate integral lines wither their values displayed below the peak. Peak signals are above their respective peak.

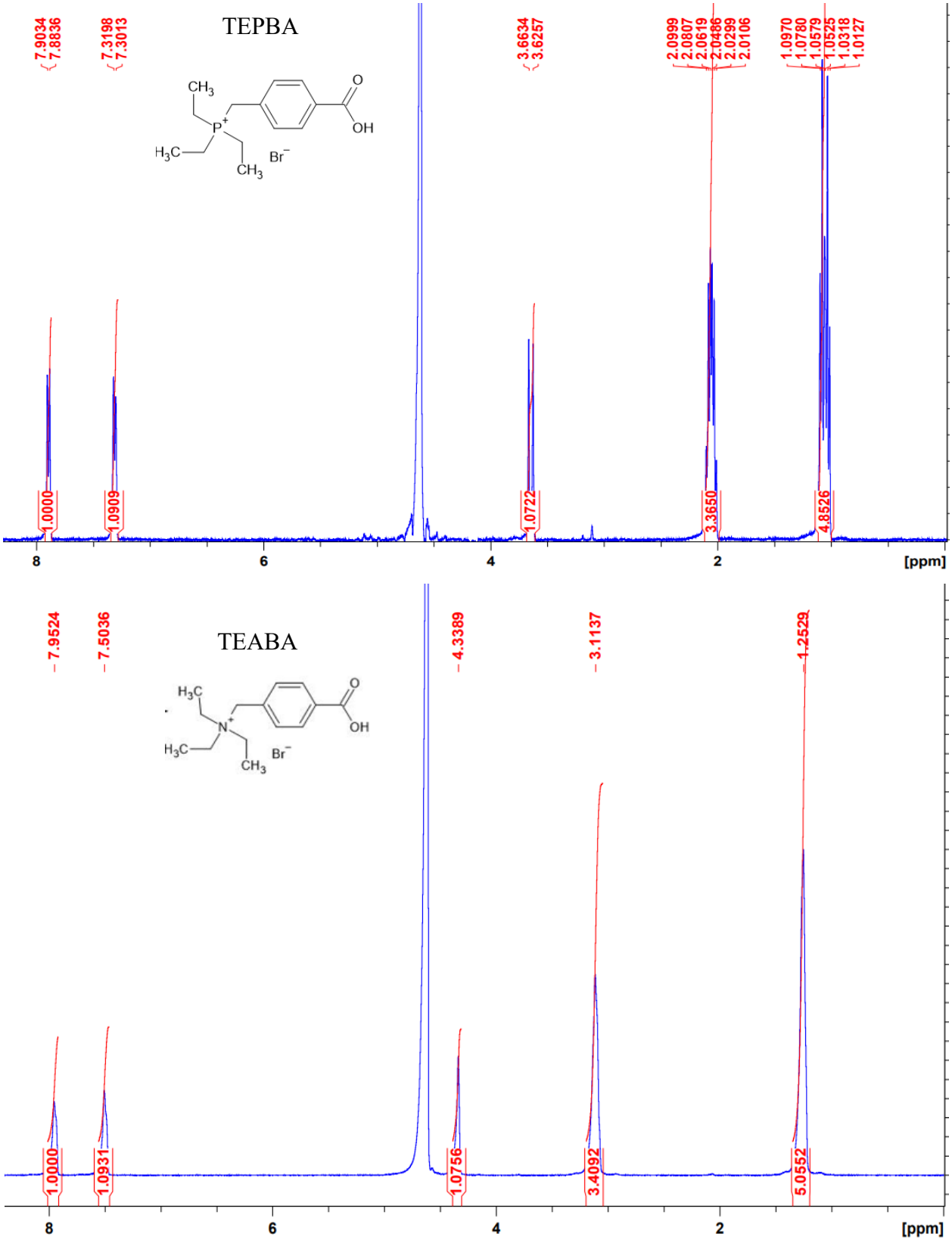

Figure 8. ^{1}H NMR spectra of carboxylic acid ligands in DMSO.

Both sets of spectra show benzene ring peaks between 7.40 and 7.85 ppm (2H). The peaks between 4.00 and 3.20 ppm correspond to the protons found on the glucosamine units of chitosan. For the TEABA-CS, the peak at 3.16 ppm (2H) represents the methylene peak between benzene and the ammonium group (-C**H**$_2$N$^+$(CH$_2$CH$_3$)$_3$). The peak at 2.70 ppm (6H) represents the first carbon on the ethyl chain after the N$^+$ (-N$^+$(C**H**$_2$CH$_3$)$_3$). Peaks for the end of the ethyl chain are at 1.30 ppm (9H). For TEPBA-CS, the methyl peak shows up at 2.72 ppm (2H). The peak at 2.19 ppm (6H) correspond to the first carbon in the ethyl chain after phosphonium (-P$^+$(C**H**$_2$CH$_3$)$_3$). The final peak at 1.19 ppm (9H) correspond to the final hydrogens on the ethyl chain. Figure 9 displays the spectra for both chitosan derivatives.

The degree of substitution (DS) could also be determined using the ^{1}H NMR spectra for each compound. Since all of the compounds contained peaks for the terminal hydrogens on the quarternary group (-X$^+$(CH$_2$C**H**$_3$)$_3$), the integral value for those peaks can be divided by 9. This would then give the integral value for 1 hydrogen on that group. The same can be done with the chitosan peak from 4.00-3.20 ppm. In this case, there are 6 hydrogens that are present in one glucosamine unit. By dividing the total integration value of those peaks by 6, a single hydrogen value can be obtained. Taking the value for the terminal hydrogen integration value and dividing it by the glucosamine units integration value and multiplying by 100 gives the degree of substitution. In other words, this number explains how many glucosamine units have the carboxylic acid ligands attached to them. Figure 10 features the equation used to find the DS of all the chitosan derivatives that were studied. These values were then compared to determine if the DS could be manipulated to by changing the amount of acid ligand that was used in the reaction. Table 2 contains all the DS values for each compound synthesized in this work.

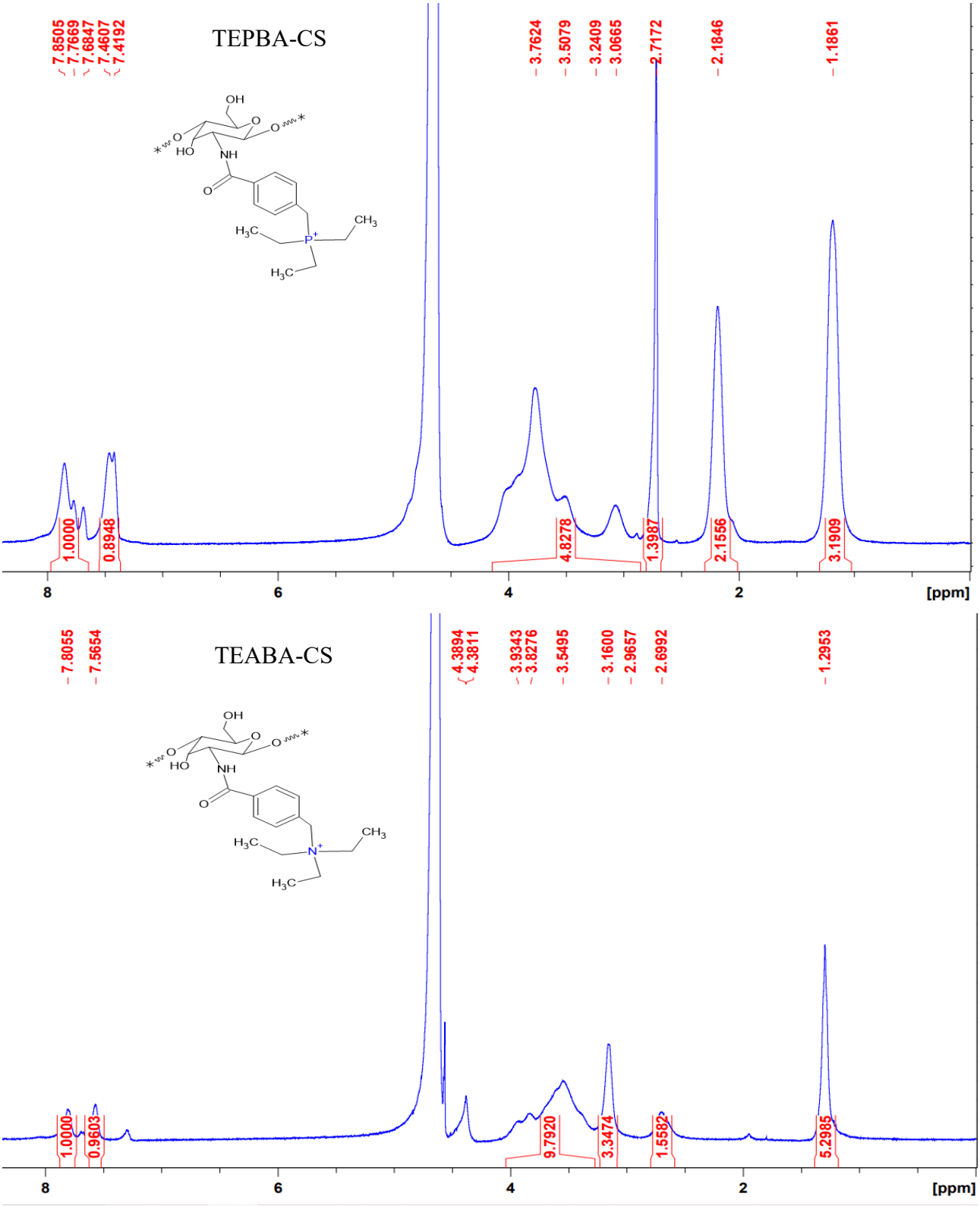

Figure 9. ^{1}H NMR spectra of carboxylic acid substituted chitosan derivatives in D_2O.

$$DS = \frac{I_s \div H_s}{\sum I_{chitosan(4.0-3.3\ ppm)} \div 6}$$

Figure 10. Equation used for calculating the degree of substitution where I_s is the integrated signal value for the carboxylic acid ligand, H_s is the number of protons associated to the ligand, and $I_{chitosan}$ is the integrated signal value for chitosan protons.

Table 2. Calculated degree of substitution (DS) for all chitosan derivatives.

Compound	Molar Ratio (acid:chitosan)	Degree of Substitution (DS)	Yield (mg)	% Recovery
TEPBA-CS-4	1:1	16.8%	200	26.7
TEPBA-CS-7	1:1	28.1%	362	32.9
TEPBA-CS-5	2:1	16.0%	130	52.0
TEPBA-CS-6	2:1	28.7%	237	94.8
TEPBA-CS-3	2:1	21.9%	394	78.8
TEPBA-CS-8	2:1	23.8%	277	50.3
TEPBA-CS-10	2:1	22.6%	626	79.2
TEPBA-CS-11	2:1	34.2%	38	2.8
TEABA-CS-1	2:1	33.1%	221	88.4
TEABA-CS-2	1:1	25.8%	194	22.4
TEABA-CS-4	1:1	14.8%	459	62.4
TEABA-CS-5	3:1	25.0%	185	25.8
TEABA-CS-6	3:1	17.6%	586	49.5
TEABA-CS-7	3:1	21.6%	675	69.7
TEABA-CS-8	5:1	28.2%	220	37.8

As can be seen from Table 2, it seems that the degree of substitution was not dependent on the amount of acid added to the reaction mixture. In many cases, it was difficult to get a consistent number with identical runs. This means that there must be other factors involved in the DS that don't include the acid ligand. Unfortunately, the DS could not be controlled through changing the ratio of acid ligand to chitosan to any reasonable degree.

3.1.3. PEGylated Chitosan Derivatives. TEAB-CS and TEPB-CS were PEGylated as discussed in the Experimental Methods section and studied using ^{1}H NMR to determine addition of mPEG to chitosan. Both spectra show the addition of mPEG into chitosan as 3.54 ppm and 3.37 ppm for TEAB-CS-mPEG and TEPB-CS-mPEG respectively. The DS for the mPEG attached to chitosan was also calculated. This was done by calculating the integral value for one methyl proton at around 1.1 ppm for both compounds. The integration value for the six chitosan protons on the substituted derivative was calculated using percent substitutions calculated by Wyatt. The integral values for the six chitosan protons and the corresponding integration values for the 12 protons on the TEAB group were subtracted from the total integration value from 2.60-4.00 ppm to obtain the integration value for mPEG. The percent substitution for mPEG was then calculated by comparing the integration value for one mPEG proton with that of chitosan. For TEPB-CS-g-mPEG the DS of mPEG was 2.6% and TEAB-CS-g-mPEG was 3.1%. Figure 11 shows the spectra of these two PEGylated derivatives.

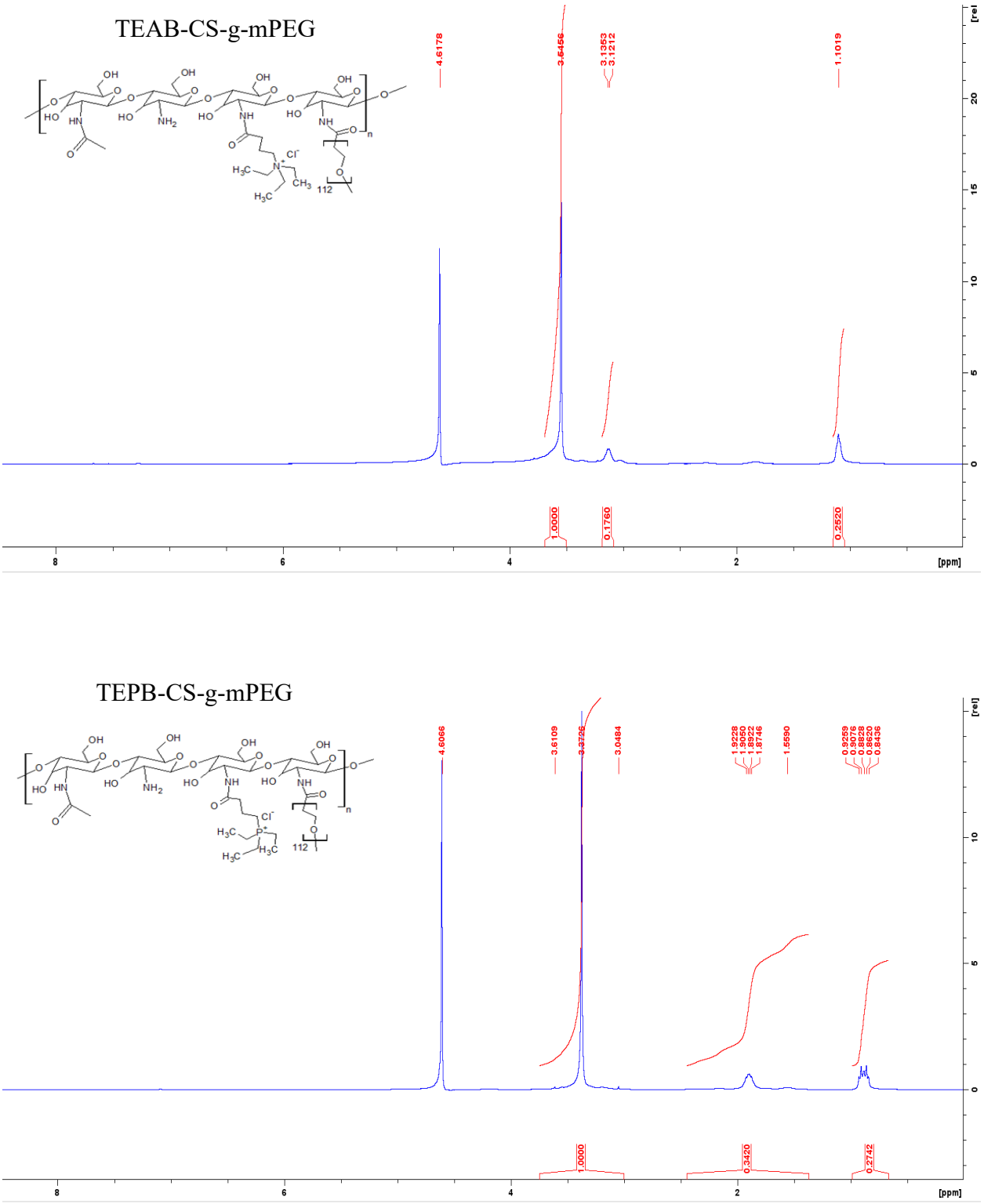

Figure 11. ^{1}H NMR spectra of PEGylated TEAB-CS and TEPB-CS in D_2O

3.2. FT-IR Analysis

FT-IR analysis was conducted on two different chitosan derivatives to determine changes in the spectra after attachment of the carboxylic acid ligand. 95% deacetlyated chitosan was also analyzed as a control. Peaks at wavenumbers near 1640 cm^{-1} and 1550 cm^{-1} were observed for both ammonium and phosphonium derivatives, indicating that amide bond formation had occurred between chitosan and the ligands. $C\text{-}N^{+}$ stretching was observed for the ammonium chitosan derivative near wavenumber 1450 cm^{-1} consistent with findings from Tan et al.[31] $C\text{-}P^{+}$ stretching for the phosphonium derivative was observed near wavenumber 1451 cm^{-1} consistent with those found by Qian et al.[58] Peaks observed from 3440-3420 cm^{-1} are assigned to the hydroxyl and amino groups found on the glucosamine units of chitosan. C-H stretching was observed for chitosan and the two derivatives around wavenumber 2920 cm^{-1}, although the ammonium derivative seems to have a less prominent peak at this position. Peaks at wavenumbers near 1650 cm^{-1} are associated to the C=O stretching vibrations from the amide bonds. N-H bending vibrations from the amides are at 1550 cm^{-1}. C-O stretching from carbons on the chitosan ring were observed at wavenumbers 1099-1074 cm^{-1}. Figure 12 shows all the spectra overlayed to help compare chitosan to the derivatives. Individual spectra are found in Appendix B.

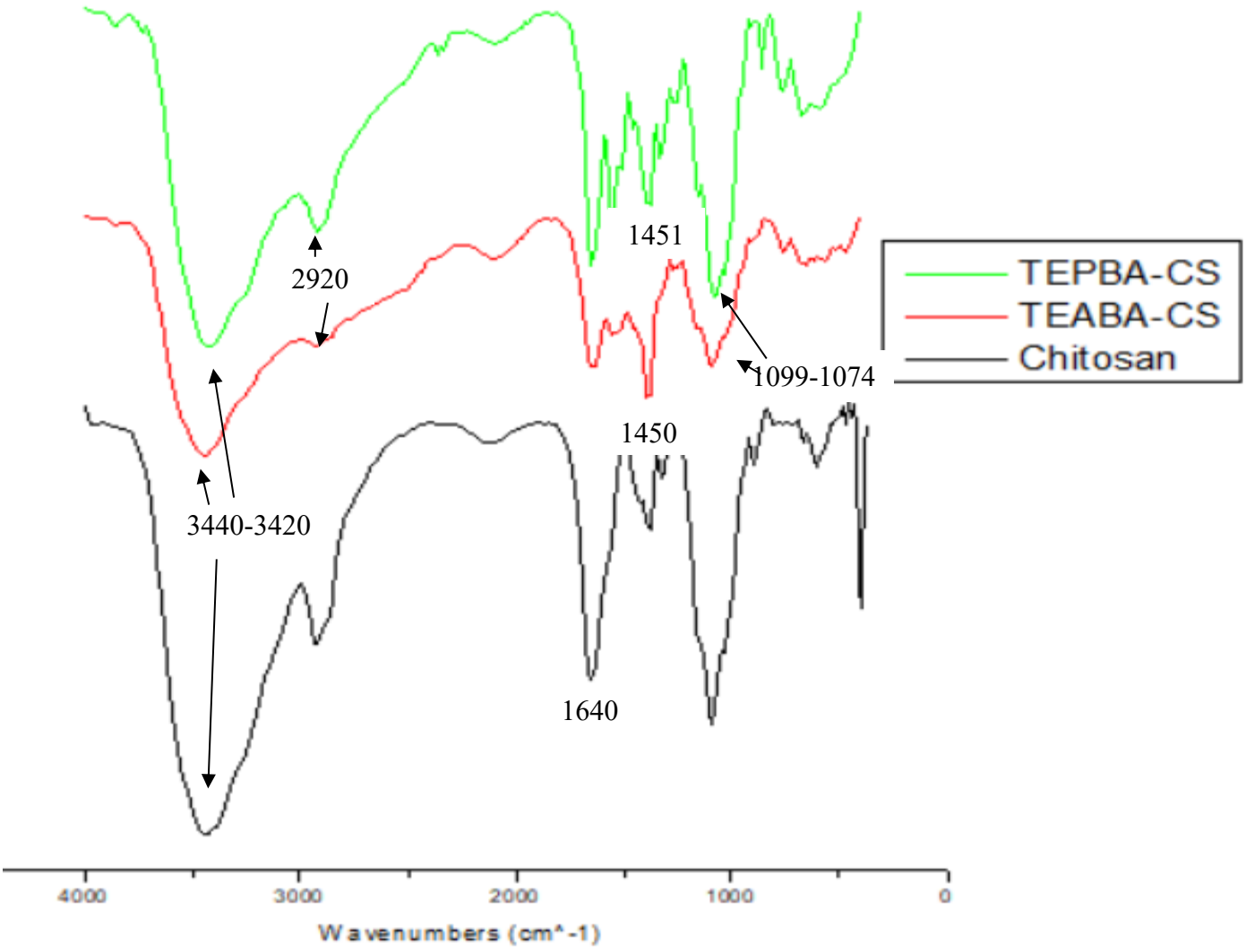

Figure 12. FT-IR spectra of chitosan, TEABA-CS, and TEPBA-CS.

3.3. Agarose Gel Electrophoresis

Agarose gel electrophoresis was conducted to determine concentrations at which the chitosan derivatives would completely complex with pDNA. The concentration of pDNA was 187 µg/mL with 3,792 base pairs provided by Dr. Kyoungtae Kim. Concentrations of the polymer solutions were then calculated to give charge ratios ranging from 8x-1/2x for TEABA-CS and 16x-1/4x for TEPBA-CS. Charge ratios are expressed as N^+:P^- or P^+:P^- where the

positive charge is from the chitosan derivatives and the negative charge is the phosphates on pDNA. For charge ratios above 4x, complete complexation can be observed for all chitosan derivatives synthesized in this study. This can be seen in Figure 13 by the lanes where the pDNA has not migrated out of the well. In all other wells, the pDNA moves down the gel signifying that pDNA is uncomplexed. As can be seen in Figure 13, both ammonium and phosphonium derivatives have the same interaction with pDNA at the various charge ratios. It should be noted that the derivatives used for this study were the ones with the highest DS, TEPBA-CS-11 and TEABA-CS-1. Since both compounds had a DS between 33% and 34% they compare quite well.

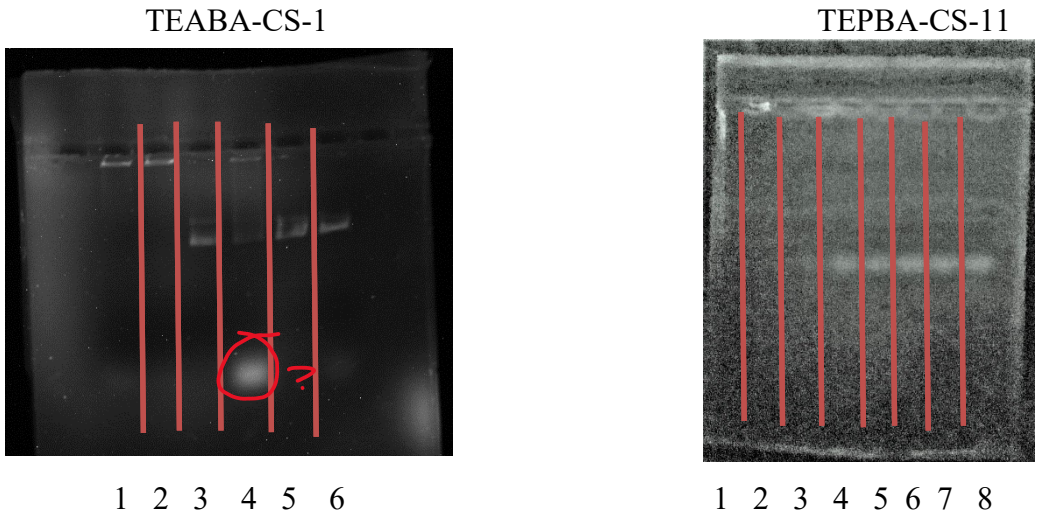

Figure 13. Agarose gel electrophoresis results for TEABA-CS-1 and TEPBA-CS-11. TEABA-CS-1 charge ratios are as follows: Lane 1 (8:1), Lane 2 (4:1), Lane 3 (2:1), Lane 4 (1:1), Lane 5 (1/2:1), Lane 6 (naked pDNA). TEPBA-CS-11 charge ratios are as follows: Lane 1 (16:1), Lane 2 (8:1), Lane 3 (4:1), Lane 4 (2:1), Lane 5 (1:1), Lane 6 (1/2:1), Lane 7 (1/4:1), Lane 8 (naked pDNA). Weight ratios were also determined. TEABA-CS-1 weight ratios are as follows: Lane 1 (2.80:1), Lane 2 (1.35:1), Lane 3 (0.67:1), Lane 4 (0.33:1), Lane 5 (0.17:1), Lane 6 (naked pDNA). TEPBA-CS-11 weight ratios are as follows: Lane 1 (4.60:1), Lane 2 (2.80:1), Lane 3 (1.35:1), Lane 4 (0.67:1), Lane 5 (0.33:1), Lane 6 (0.17:1), Lane 7 (0.09:1), Lane 8 (naked pDNA).

Gel electrophoresis was also run on TEAB-CS and TEPB-CS. In those cases, the compounds show complete interaction with DNA at charge ratios at 4x or higher. This translates to a weight ratio of 1.35 polymer to DNA. Figure 14 shows the results in terms of charge ratio and weight ratios. It is interesting to note that both PEGylated and non-PEGylated compounds show the same results. PEGylation would seem to not have any effect on the interaction of chitosan with pDNA with these derivatives.

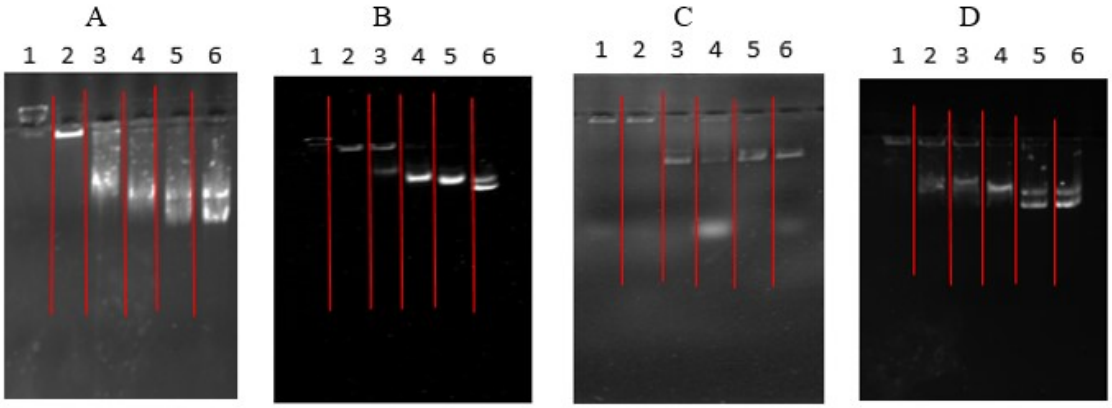

Figure 14. pDNA-binding ability of TEAB-CS (A), TEAB-CS-g-mPEG (B), TEPB-CS (C), and TEPB-CS-g-mPEG (D). Electrophoretic mobility of pDNA with the chitosan derivatives at N^+/P^- and P^+/P^- ratios: Lane 1 (8:1 ratio), Lane 2 (4:1), Lane 3 (2:1), Lane 4 (1:1), Lane 5 (1/2:1), and Lane 6 (naked pDNA)

3.4. Circular Dichroism (CD)

CD analysis was used to observe electrostatic interaction with calf thymus DNA and chitosan derivatives. For these studies, the compounds TEAB-CS, TEPB-CS, TEAB-CS-g-mPEG, and TEPB-CS-g-mPEg synthesized were studied in great detail. CD spectra for B-form double-stranded DNA was first measured. Varying amounts of polymer were then added to the DNA to see how the spectra would change. It's important to note that chitosan and the derivatives studied do not produce a signal in the wavelengths studied. In the calf thymus DNA,

there are positive and negative ellipticities that are centered around 280 nm (positive) and 250 nm (negative). These findings are in accordance with literature values found for B-form DNA.[59,61,62] Figure 15 shows the CD spectra of calf DNA along with the different derivatives studied. For this figure, the concentration of the polymer is 4x the amount of DNA. In previous work, it was discovered that these compounds fully complex at these concentrations. As can be seen in Figure 15, the compound that changes the conformation of B-DNA is TEAB-CS. It is also worth noting that the mPEG versions of each derivative don't seem to have the same effect as their un-peglyated versions. The compound that has the least effect on the conformation of the DNA is TEPB-CS, indicating that it would perhaps be the best candidate for further studies with cytotoxicity. As the weight ratios of each compound are increased the conformational change to DNA is drastic. This indicates that the compounds are interacting with DNA but are also denaturing it. CD analysis indicates that the compounds are interacting with DNA at concentrations that agree with Wyatt's previous results. For every compound, even at just weight ratios of 2:1 polymer to DNA, there is a slight change in the CD spectra indicating that conformational changes are occurring. The largest difference comes around weight ratios 4 and 8 where the positive and negative ellipticities are almost completely flattened.

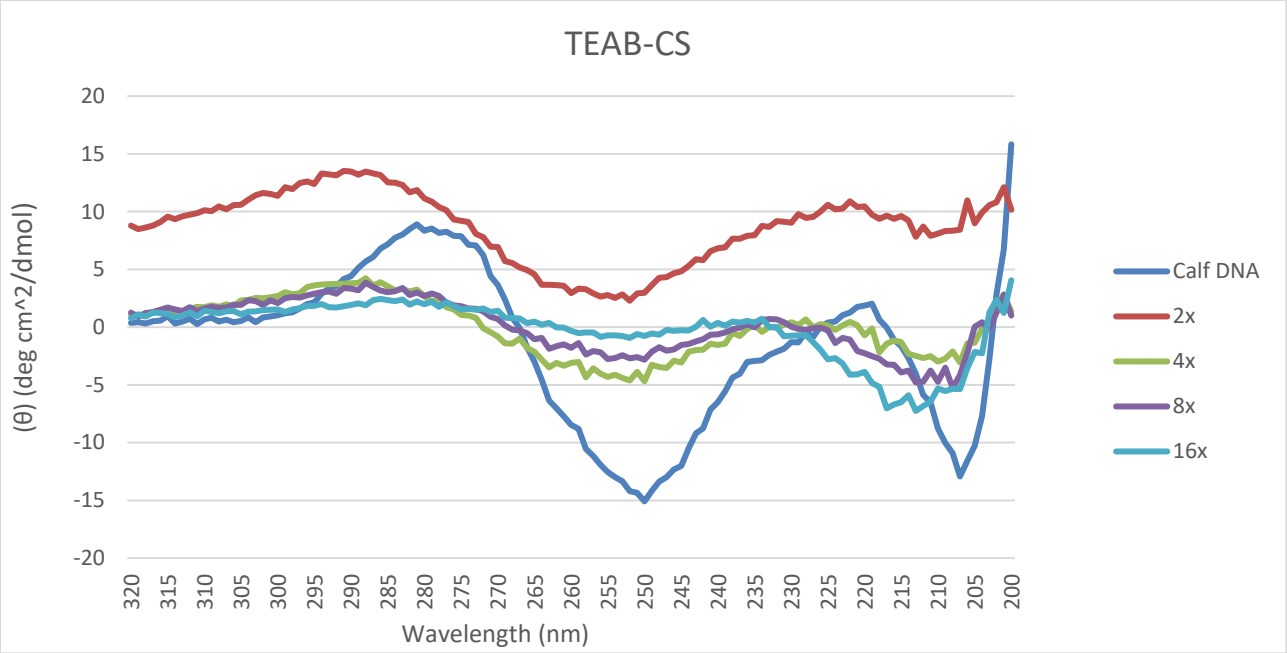
TEAB-CS
(θ) (deg cm^2/dmol)
Wavelength (nm)
Calf DNA
2x
4x
8x
16x

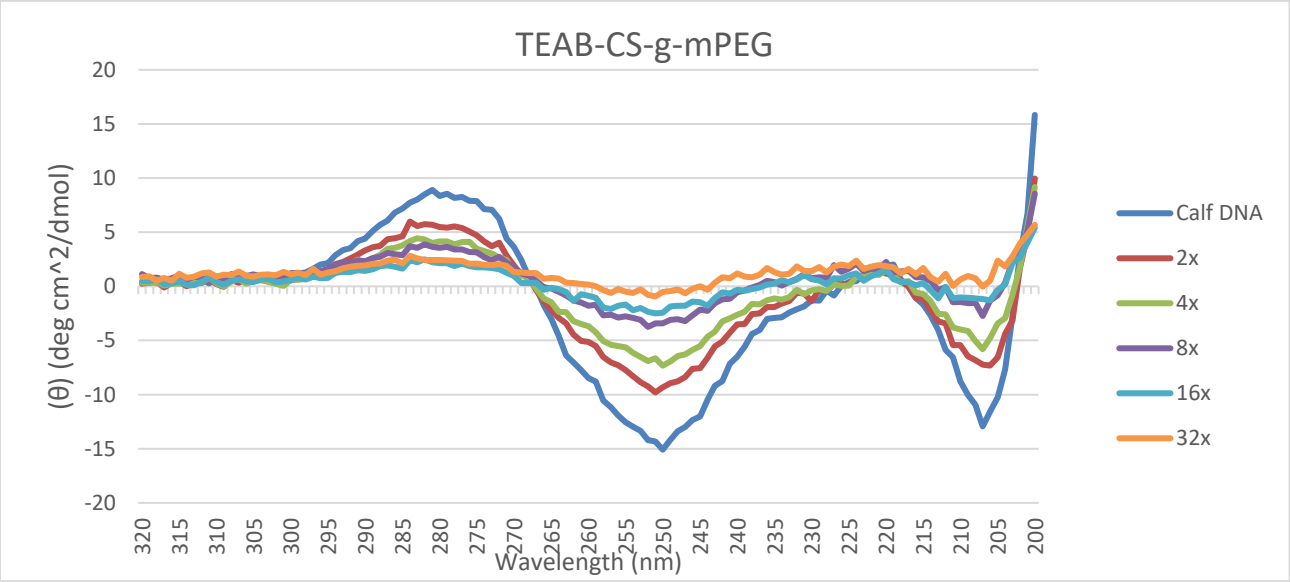
TEAB-CS-g-mPEG
(θ) (deg cm^2/dmol)
Wavelength (nm)
Calf DNA
2x
4x
8x
16x
32x

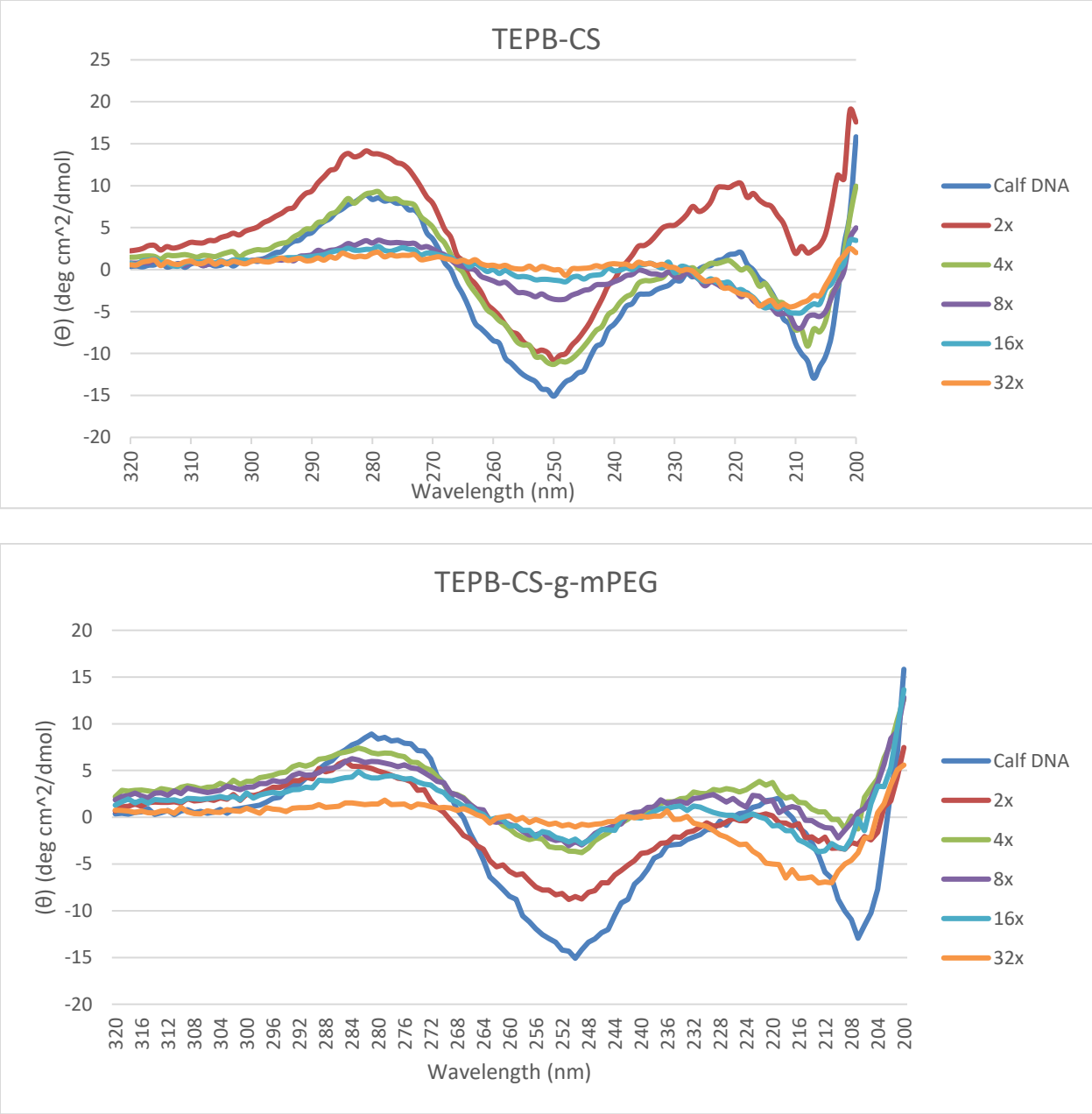

Figure 15. CD spectra of Calf Thymus DNA interacting with chitosan derivatives.

3.5. Dynamic Light Scattering (DLS) Size Determination

DLS measurements were taken in order to confirm that the DNA/polymer complex (polyplex) would be small enough to enter cells and be efficient gene therapy vectors. Cells usually uptake polyplexes ranging from 50 to several hundred nanometers.[63] Polyplexes were

formed in both water and phosphate buffer saline solution (PBS) at pH 7.4. Increasing amounts of polymer were added to determine optimal size. Ratios for the experiments were done in DNA:Polymer weight ratios ranging from 1:1 to 1:10. Experiments were run in triplicate and averaged to determine size. Standard deviations for each measurement were also calculated. Table 3 shows the results for the polyplexes in water while Table 4 represents runs in PBS.

TEAB-CS has the smallest polyplexes when compared to the other compounds. However, increasing the weight ratios of all polymers leads to an increase in hydrodynamic diameter. This could be due to the hydration of counter ions associated with the polycations which results in swelling of the nanoparticles. These results are comparable to those found in literature.[63] Polyplexes formed from quarternized cellulose with pDNA at N/P ratios of 1:1 gave sizes in the range of 1380 and 1070 nm, but increasing the N/P ratios resulted in particle sized in the range of about 400-500 nm.[64] It is also interesting to note that the standard deviations for measurements in PBS were smaller. This could be due to the controlled pH of the buffer solution keeping the DNA in a stable state. In the water measurements, distilled, deionized water was used so slight changes to pH from chitosan compounds could drastically change the pH of the system. DLS measurements were able to confirm that the polyplexes formed by the chitosan derivatives and calf DNA are small enough to enter cells.

Table 3. Size of DNA/Polymer Complexes in Water

DNA:Polymer Weight Ratio	TEAB-CS	TEAB-CS-g-mPEG	TEPB-CS	TEPB-CS-g-mPEG
1:1	141 ± 31	234 ± 21	262 ± 30	250 ± 42
1:2	193 ± 26	268 ± 16	200 ± 30	309 ± 9
1:3	197 ± 33	252 ± 25	282 ± 45	233 ± 23

Table 4. Size of DNA/Polymer Complexes in PBS at pH 7.4

DNA:Polymer Weight Ratio	TEAB-CS	TEAB-CS-g-mPEG	TEPB-CS	TEPB-CS-g-mPEG
1:1	190 ± 9	168 ± 4	186 ± 7	206 ± 22
1:2	210 ± 10	186 ± 2	252 ± 14	248 ± 9
1:3	221 ± 13	242 ± 32	245 ± 24	252 ± 9
1:4	254 ± 30	259 ± 4	268 ± 11	256 ± 31
1:5	236 ± 10	322 ± 7	320 ± 24	333 ± 19
1:10	282 ± 8	277 ± 2	304 ± 9	333 ± 12

3.6. Zeta Potential

Zeta potential measurements were taken to determine complete complexation between chitosan derivatives and calf thymus DNA. Measurements were taken with a Brookhaven NanoBrook Omni particle analyzer with a scattering angle of 173º. Final concentration of DNA in the 1.5 mL sample cell was 15 µg/mL. Increasing amounts of polymer were then added to the DNA in weight ratios from 1:1 to 8:1 (polymer:DNA). Polymers used for this experiment were TEAB-CS, TEPB-CS, TEPB-CS-g-mPEG, and TEAB-CS-g-mPEG. The results can be seen in Figure 16. All compounds start around 35 mV to -30 mV. As the ratio moves to 2:1, the pegylated compounds have a huge jump to around -10 mV to -5 mV while the unpeglyated compounds stay relatively unchanged at around -30 mV to -25 mV. When the ratio is 3:1, all compounds have zeta potentials that become positive indicating that the DNA and polymer are at equal N^+/P^- or P^+/P^- charge ratios and have complexed. Once the ratio has gone above 4:1 there is a plateau of the zeta potential for each zeta potential. The pegylated compounds seem to plateau at a lower zeta potential which is probably due to the mPEG reducing the charge of the

quarternary groups attached to chitosan. All compounds studied in this experiment show complete condensation with DNA at a weight ratio of 3:1. Adding polymer past this ratio results in positive zeta potentials resulting in complete complexation of DNA with extra polymer that does not interact with DNA.

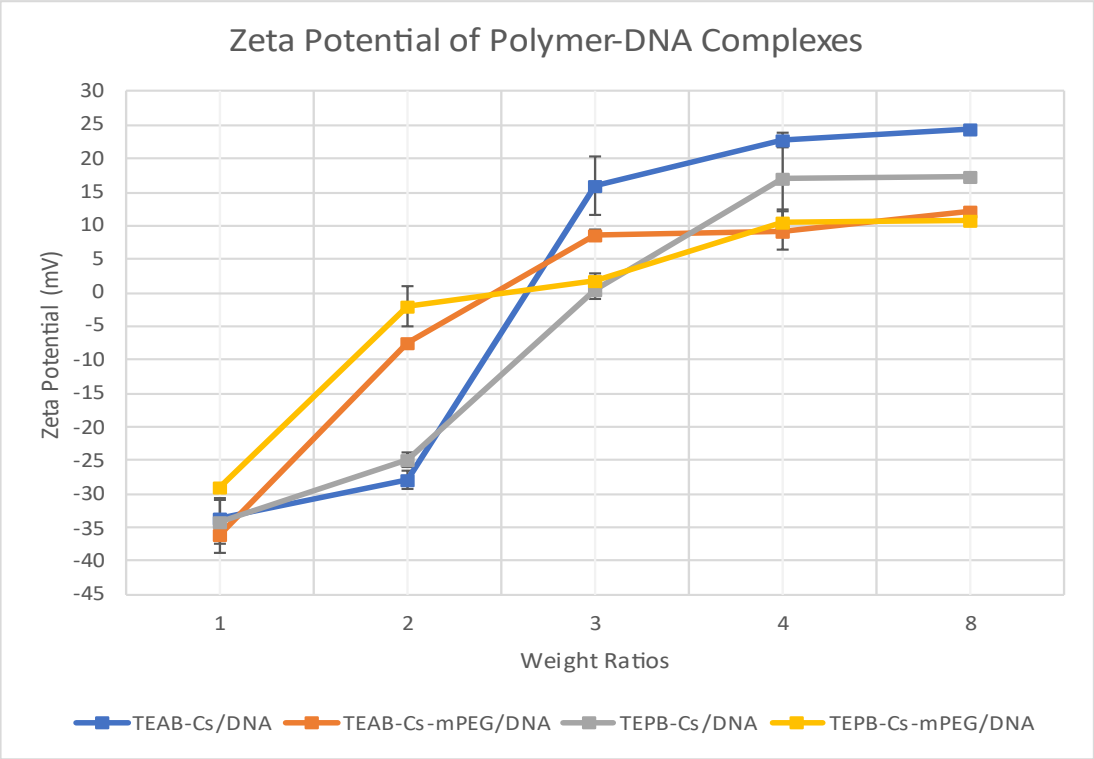

Figure 16. Zeta potentials for DNA/polymer complexes. Measurements were taken in triplicate and error bars are shown for the standard deviation of each point.

3.7. Solubility Studies

Solubility studies were conducted on TEAB-CS, TEPB-CS, TEAB-CS-g-mPEG, and TEPB-CS-g-mPEG to determine if the addition of the ammonium and phosphonium groups aided in making chitosan soluble in neutral aqueous media. Figure 17 shows the results for the studies. It was found that for each compound, even the PEGylated ones, that they were soluble in all conditions up to pH 10. Further pH increases were not recorded as physiological pH is 7.4

and the study went well above that. Chitosan was also tested as a control and found that it crashes out of solution at around pH 6.

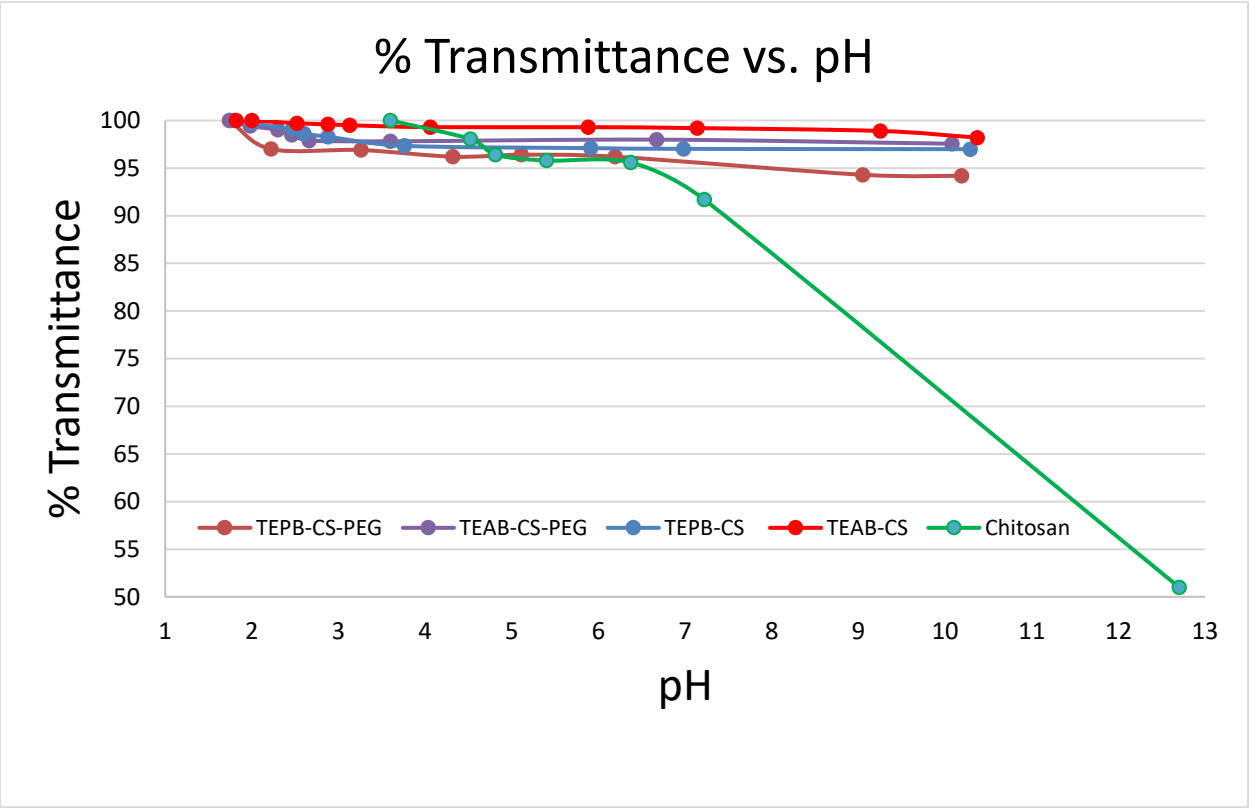

Figure 17. %T versus pH for chitosan derivatives.

CHAPTER 4. CONCLUSION

In this work, ammonium and phosphonium substituted chitosan derivatives were synthesized with the goal of making chitosan more soluble in neutral pH. The compounds were also designed to interact with DNA to be efficient vectors for gene therapy uses. The degree of substitution for each compound was determined using ^{1}H NMR and found that altering the amount of acid added to chitosan had no effect on the degree of substitution. Most of the compounds had degree of substitution around 16-30%. ^{1}H NMR was also used to determine if complete reaction had occurred between chitosan and the carboxylic acid ligand. FT-IR analyses also aided in determining complete conjugation of the ligands to chitosan. Agarose gel electrophoresis showed that these novel chitosan derivatives do interact with pDNA at charge ratios of 4x for both ammonium and phosphonium derivatives. Further work on the compounds TEABA-CS and TEPBA-CS should be conducted in regard to size and zeta potential measurements. Cytotoxicity studies should also be conducted.

The compounds synthesized by Wyatt, TEPB-CS and TEAB-CS, as well as the PEGylated versions of these compounds were studied with agarose gel electrophoresis as well. It was found that these compounds also interact with DNA at charge ratios of 4x that of DNA. Solubility studies show that even at pH near 10 that these compounds are soluble. DLS measurements were conducted to determine polyplex size. It was found that they are in the 200-400 nm range and can enter cells easily at this size. Zeta potentials were also conducted for these derivatives to determine when complete complexation had occurred. All compounds at a weight ratio of 3x that of DNA showed zeta potentials at zero or positive meaning that complexation had occurred. CD analysis also determined that at these compounds at weight

ratios 4x those of DNA started to change the conformation of the DNA. Cytotoxicity studies and transfection efficiency had been previously studied on these compounds, so the work with Wyatt's derivatives is concluded.

REFERENCES

(1) Tang, W.; Fernandez, J.; Sohn, J.; Amemiya, C. Chitin Is Endogenously Produced in Vertebrates. *Curr Biol* **2015**, *25* (7), 897–900.

(2) Peniston, Q. Process for the Manufacture of Chitosan. *Key Engineering Materials* **2006,** *4*, 175-195.

(3) Kas, H. S. Chitosan: Properties, Preparations and Application to Microparticulate Systems. *J. Microencapsul.* **1997**, *14*, 689–711.

(4) Hussain, M. R. Determination of Degree of Deacetylation of Chitosan and Their Effect on the Release Behavior of Essential Oil from Chitosan and Chitosan-Gelatin Complex Microcapsules. *IJA-ERA* **2013**, *6* (4), 4–12.

(5) No, H. K.; Meyers, S. P. Preparation and Characterization of Chitin and Chitosan-a Review. *J. Aquat. Food Prod. Technol.* **1995**, *4* (2), 27–52.

(6) Chung, T. W.; Lu, Y. F.; Wang, H. Y.; Chen, W. P.; Wang, S. S.; Lin, Y. S.; Chu, S. H. Prediction Models of Long-Term Cirrhosis and Hepatocellular Carcinoma Risk in Chronic Hepatitis B Patients: Risk Scores Integrating Host and Virus Profiles. *Artifical Organs* **2003**, *27*, 155–161.

(7) Ogawa, K.; Yui, T.; Okuyama, K. Three-D Structures of Chitosan. *Int. J. Biol. Macromol.* **2004**, *34* (1), 1–8.

(8) Abbas, A. M. Iowa Health Focus. *Iowa Research Online*. 2010, pp 1–365.

(9) Singla, A. K.; Chawla, M. Chitosan: Some Pharmaceutical and Biological Aspects - an Update. *J. Pharm. Pharmacol.* **2001**, *53*, 1047–1067.

(10) Argin-Soysal, S.; Kofinas, P.; Lo, Y. Effect of Complexation Conditions on Xanthan-Chitosan Polyelectrolyte Complex Gels. *Food Hydrocoll.* **2009**, *23*, 202–209.

(11) Kiang, T.; Wen, J.; Lim, H.; Leong, K. Novel Thermally Sensitive PH-Dependent Chitosan/ Carboxymethyl Cellulose Hydrogels. *Biomaterials* **2004**, *25*, 5293–5301.

(12) Koping-Hoggard, M.; Melnikova, Y.; Varum, K.; Lindman, B.; Artursson, P. Improved Chitosan-Mediated Gene Delivery Based on Easily Dissociated Chitosan Polyplexes of Highly Defined Chitosan Oligomers. *J. Gene Med. 5* (2), 130–141.

(13) Lee, K.; Ha, W.; Park, W. Synthesis and Characterization of Chitosan/Gum Arabic Nanoparticles for Bone Regeneration. *Biomaterial* **1995**, *16*, 1211–1216.

(14) Aiba, S. Studies on Chitosan: 4. Lysozymic Hydrolysis of Partially N-Acetylated Chitosan. *Int. J. Biol. Macromol.* **1992**, *16*, 225–228.

(15) Margolis, H. Tycho's Illusion and Human Cognition. *Nature* **1998**, *392*, 857.

(16) Templeton, N. Gene and Cell Therapy Based Treatment Strategies for Inflammatory Bowel Disease. *Gene Cell Ther.* **2015**, 1271–1310.

(17) Scanlon, K. Cancer-Specific Gene Therapy. *Cancer Gene Ther.* **2004**, *11*, 841.

(18) Flotte, T. Gene Therapy: The First Two Decades and the Current State-of-the-Art. *J. Cell. Physiol.* **2007**, *213*, 301–305.

(19) Santos-Carballal, B.; Fernandez, E. F.; Goycoolea, F. Chitosan in Non-Viral Gene Delivery: Role of Structure, Characterization Methods, and Insights in Cancer and Rare Diseases Therapies. *Polymers 10* (4), 1–51. https://doi.org/10.3390/polym10040444.

(20) Lundstrom, K.; Boulikas, T. Viral and Non-Viral Vectors in Gene Therapy: Technology Development and Clinical Trials. *Technol. Cancer Res. Treat.* **2003**, *2*, 471–485.

(21) Ravi Kumar, M.; Muzzarelli, R.; Muzzarelli, C.; Sashiwa, H. Chitosan Chemistry and Pharmaceutical Perspectives. *Chem. Rev.* **2005**, *104* (12), 6017–6084.

(22) Jiang, X.; Dai, H.; Leong, K.; Goh, S.; Mao, H.; Yang, Y. Chitosan-g-PEG/DNA Complexes Deliver Gene to the Rat Liver via Intrabiliary and Intraportal Infusions. *J. Gene Med.* **2006**, *8*, 477–487.

(23) Weber, P.; Wendoloski, J.; Pantoliano, M.; Salemme, F. Crystallographic and Thermodynamic Comparison of Natural and Synthetic Ligands Bound to Streptavidin. *J. Am. Chem. Soc.* **1992**, *114*, 3197–3200.

(24) Nakajima, N.; Ikada, Y. Mechanism of Amide Formation by Carbodiimide for Bioconjugation in Aqueous Media. *Bioconjug. Chem.* **1995**, *6*, 123–130.

(25) Kim, Y.; Gihm, S.; Park, C.; Lee, K.; Kim, T.; Kwon, I.; Chung, H.; Jeong, S. Structural Characteristics of Size-Controlled Self-Aggregates of Deoxycholic Acid-Modified Chitosan and Their Application as a DNA Delivery Carrier. *Bioconjug. Chem.* **2001**, *12*, 932–938.

(26) Tang, Y.; Cummins, J.; Huard, J.; Wang, B. The Susceptibility of Muscle Cells to Oxidative Stress Is Independent of Nitric Oxide Synthase Expression. *Expert Opin. Biol. Ther.* **2010**, *10*, 395–408.

(27) Wyatt, Q. Synthesis, Characterization, and Applications of Ammonium/Phosphonium Chitosan Derivatives for Investigative DNA Interactions, Missouri State University, Master's Thesis, **2018,** Springfield, MO.

(28) Yeomans, D.; Wilson, S. Herpes Virus-Based Recombinant Herpes Vectors: Gene Therapy for Pain and Molecular Tool for Pain Science. *Gene Ther.* **2009**, *16*, 502–508.
(29) Stevens, M. *Polymer Chemistry An Introduction*; Oxford University Press.

(30) Chalikonda, S.; Bartlett, D. Cancer Drug Resistance: An Evolving Paradigm. *Cancer Drug Discov. Dev. Gene Ther. Cancer* **2004**, 73–85.

(31) Tan, W.; Zhang, J.; Luan, F.; Wei, L.; Chen, Y.; Dong, F.; Li, Q.; Guo, Z. Investigation of the Properties of N-[(2-Hydroxy-3-Trimethylammonium) Propyl] Chloride Chitosan Derivatives. *Int. J. Biol. Macromol.* **2017**, *102*, 704–711.

(32) Dou, X. Synthesis, Characterization, and Applications of Dendrimers, Missouri State University, Master's Thesis, **2015**, Springfield, MO.

(33) Lu, Y.; Madu, C. The Biological Routes of Gene Delivery Mediated by Lipid-Based Non-Viral Vectors. *Expert Opin. Drug Deliv.* **2009**, *7*, 19–35.

(34) Schmidt-Wolf, G.; Schmidt-Wolf, I. Engineering a Serum-Resistant and Thermostable Vesicular Stomatitis Virus G Glycoprotein for Pseudotyping Retroviral and Lentiviral Vectors. *Trends Mol. Med.* **2003**, *9*, 67–72.

(35) Gao, X.; Kim, K.; Liu, D. Intracellular Gene Transfer in Rats by Tail Vein Injection of Plasmid DNA. *AAPS J.* **2010**, *12* (4), 692–698.

(36) Jaidee, A.; Rachtanapun, P.; Luangkamin, S. Antioxidant and Moisturizing Properties of Carboxymethyl Chitosan with Different Molecular Weights. *Adv. Mater. Res.* **2012**, *506*, 158–161.

(37) Koping-Hoggard, M.; Varum, K.; Issa, M.; Danielsen, S.; Christensen, B.; Stokke, B.; Artursson, P. Relationship between the Physical Shape and the Efficiency of Oligomeric Chitosan as a Gene Delivery System in Vitro and in Vivo. *Gene Ther.* **2004**, *11*, 1441–1452.

(38) Dhulipala, V.; Maddali, K.; Welshons, W.; Reddy, C. Inhibition of Human Embryonic Palatal Mesenchymal Cell Cycle by Secalonic Acid D: A Probable Mechanism of Its Cleft Palate Induction. *Birth Defects Res. B. Dev. Reprod. Toxicol.* **2005**, *74*, 233–242.

(39) Boussif, O.; Lezoualch, F.; Zanta, M.; Mergny, M.; Scherman, D.; Demeneix, B.; Behr, J. A Versatile Vector for Gene and Oligonucleotide Transfer into Cells in Culture and in Vivo: Polyethylenimine. *Proc. Natl. Acad. Sci.* **1995**, *92*, 7297–7301.

(40) Bragonzi, A.; Dina, G.; Villa, A.; Calori, G.; Biffi, A.; Bordignon, C.; Assael, B.; Conese, M. Biodistribution and Transgene Expression with Nonviral Cationic Vector/DNA Complexes in the Lungs. *Gene Ther.* **2000**, *7*, 1753–1760.

(41) Turunen, M.; Hiltunen, M.; Ruponen, M.; Virkamaki, L.; Urtti, A.; Yla-Herttuala, S. Cardiovascular Gene Therapy. *Gene Ther.* **1999**, *6*, 6–11.
(42) Gebhart, C.; Kabanov, A. Controlled Release of Bioactive Agents in Gene Therapy and Tissue Engineering. *J. Controlled Release* **2001**, *73*, 401–416.

(43) Luo, D.; Saltzman, W. Enhancement of Transfection by Physical Concentration of DNA at the Cell Surface. *Nat. Biotechnol.* **2000**, *18*, 33–37.

(44) Godbey, W.; Wu, K.; Mikos, A. Poly(Ethylenimine)-Mediated Gene Delivery Affects Endothelial Cell Function and Viability. *Biomaterials* **2001**, *22*, 471–480.

(45) Putnam, D.; Gentry, C.; Pack, D.; Langer, R. Polymer-Based Gene Delivery with Low Cytotoxicity by a Unique Balance of Side-Chain Termini. *Proc. Natl. Acad. Sci.* **2001**, *98*, 1200–1205.

(46) Regnstrom, K.; Ragnarsson, E.; Koping-Hoggard, M.; Torstensson, E.; Nyblom, H.; Artursson, P. Suppression of Tumor Growth in H-Ras12V Liver Cancer Mice by Delivery of Programmed Cell Death Protein 4 Using Galactosylated Poly(Ethylene Glycol)-Chitosan-Graft-Spermine. *Gene Ther.* **2003**, *10*, 1575–1583.

(47) Kunath, K. Low-Molecular-Weight Polyethylenimine as a Non-Viral Vector for DNA Delivery: Comparison of Physicochemical Properties, Transfection Efficiency and in Vivo Distribution with High-Molecular-Weight Polyethylenimine. *J. Controlled Release* **2003**, *89*, 113–125.

(48) Kulikov, S.; Lisovskaya, S.; Zelenikhin, P.; Bezrodnykh, E.; Shakirova, D.; Blagodatskikh, I.; Tikhonov, V. Antifungal Activity of Oligochitosans (Short Chain Chitosans) against Some Candida Species and Clinical Isolates of Candida Albicans: Molecular Weight-Activity Relationship. *Eur. J. Med. Chem.* **2014**, *74*, 169–178.

(49) Negishi, E.; Wang, G. Negishi Coupling between α-Alkyl(Aryl)Thio Vinyl Zinc Chloride and α-Bromo Vinyl Ether: A Convergent Synthesis of 2-Alkoxy-3-Alkyl(Aryl)Thiobuta-1,3-Dienes. *Org. Lett.* **2009**, 1.

(50) Maschmeyer, G. Selection Criteria for Antifungals: The Right Patients and the Right Reasons. *Int. J. Antimicrob. Agents* **2006**, *27*, 3–6.

(51) Cowen, L.; Anderson, J.; Kohn, L. Evolution of Drug Resistance in Candida Albicans. *Annu. Rev. Microbiol.* **2002**, *56*, 139–165.

(52) Vorlfckova, M.; Sagi, J. Transitions of Poly(Dl-DC), Poly(Dl-Methyl5dC) and Poly(Dl-Bromo5dC) among and within the B-, Z-, and X- DNA Families of Conformatinos. *Nucleic Acids Res.* **1991**, *19*, 2343–2347.

(53) Je, H.; Kim, E.; Lee, J.-S.; Lee, H. Release Properties and Cellular Uptake in Caco-2 Cells of Size-Controlled Chitosan Nanoparticles. *J. Agric. Food Chem.* **2017**, *65*, 10899–10906.

(54) Kim, J.; Mondal, S.; Tzeng, S.; Rui, Y.; Al-kharboosh, R.; Kozielski, K.; Bhargave, A.; Garcia, C.; Quinones-Hinojosa, A.; Green, J. Poly(Ethylene Glycol)-Poly(Beta-Amino Ester)-Based Nanoparticles for Suicide Gene Therapy Enhance Brain Penetration and Extend Survival in a Preclinical Human Glioblastoma Orthotopic Xenograft Mode. *ACS Biomater. Sci. Eng.* **2020**, *6* (5), 2943–2955.

(55) Gohy, J.-F.; Varshney, S.; Jerome, R. Water-Soluble Complexes Formed by Poly(2-Vinylpyridinium)-Block-Poly(Ethylene Oxide) and Poly(Sodium Methacrylate)-Block-Poly(Ethylene Oxide) Copolymers. *Macromolecules* **2001**, *34* (10), 3361.

(56) Greenwood, R.; Kendall, K. Selection of Suitable Dispersants for Aqueous Suspensions of Zirconia and Titania Powders Using Acoustophoresis. *J. Eur. Ceram. Soc.* **1999**, *19* (4), 479–488.

(57) Malvern. *Zeta Potential Using Laser Doppler Electrophoresis*. **2015** https://www.malvernpanalytical.com/en/technology/zeta_potential/zeta_potential_LDE.htm.

(58) Qian, C.; Xu, X.; Shen, Y.; Li, Y.; Guo, S. Effect of Chitosan-(Poly)Nitroxides on Normal and Tumor Cells under Conditions of Induced Oxidative Stress. *Carbohydr. Polym.* **2013**, No. 97, 676–683.

(59) Wang, L.; Xu, X.; Guo, S.; Peng, Z.; Tang, T. Novel Water Soluble Phosphonium Chitosan Derivatives: Synthesis, Characterization and Cytotoxicity Studies. *Int. J. Biol. Macromol.* **2011**, *48* (2), 375–380.

(60) Kean, T.; Roth, S.; Thanou, M. Biodegradation, Biodistribution and Toxicity of Chitosan. *J. Controlled Release* **2016**, *62*, 643–653.

(61) Layek, B.; Haldar, M.; Sharma, G.; Lipp, L.; Mallik, S.; Singh, J. N-Hexanoyl, N-Octanoyl and N-Decanoyl Chitosans: Binding Affinity, Cell Uptake, and Transfection. *Mol. Pharm.* **2014**, No. 11, 982–994.

(62) Lin, W.; Hsu, W. Chitosan/Fucoidan Multilayer Nanocapsules as a Vehicle for Controlled Release of Bioactive Compounds. *Carbohydr. Polym.* **2015**, *120*, 7–14.

(63) Liu, Y.; Reineke, T. Polymer Beacons for Luminescence and Magnetic Resonance Imaging of DNA Delivery. *J. Am. Chem. Soc.* **2005**, No. 127, 3004–3015.

(64) Song, Y.; Sun, Y.; Zhang, X.; Zhou, J.; Zhang, L. The Protective Role of Selenium on the Toxicity of Cisplatin-Contained Chemotherapy Regimen in Cancer Patients. *Biomacromolecules* **2008**, No. 9, 2259–2264.

APPENDICES

Appendix A. NMR

^{1}H NMR spectra were collected using a Varian 400 MHz NMR spectrometer and plotted using Bruker TopSpin software. All spectra presented in this appendix display a ppm range of 0-14. Red lines indicate the range of integration and the values found for those integrations are below the peaks. The ppm values of all signals are indicated above the spectra.

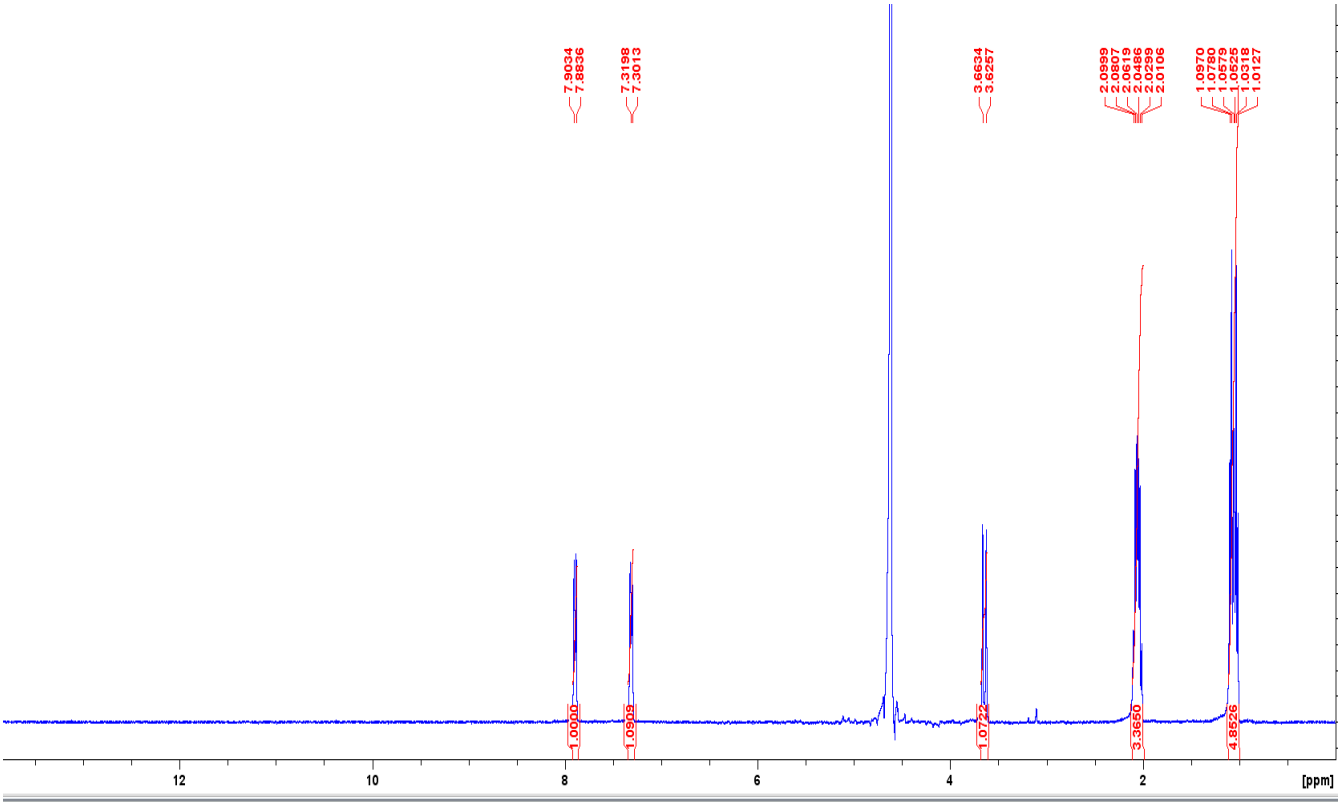

Appendix A-1. ^{1}H NMR spectrum of 4-methyltriethylphosphine benzoic acid.

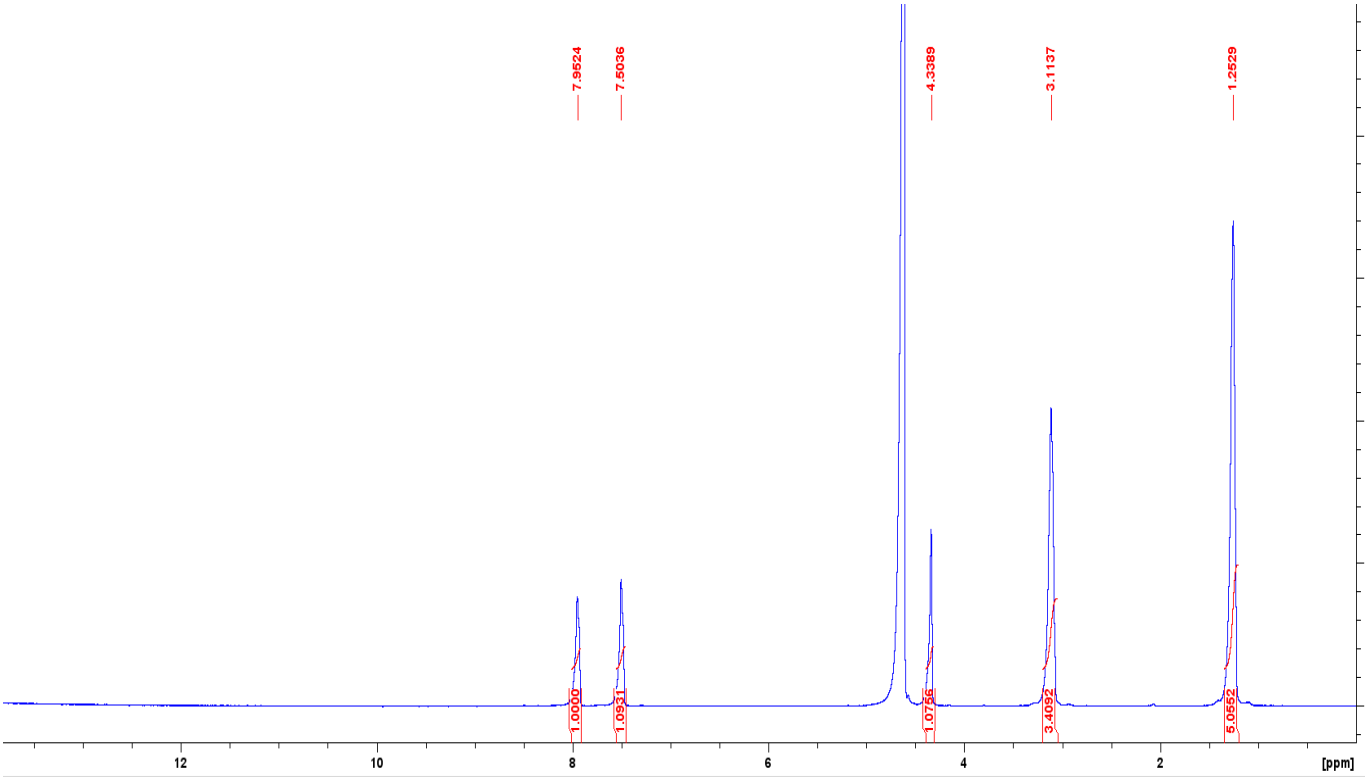

Appendix A-2. ^{1}H NMR spectrum of 4-methyltriethylamine benzoic acid.

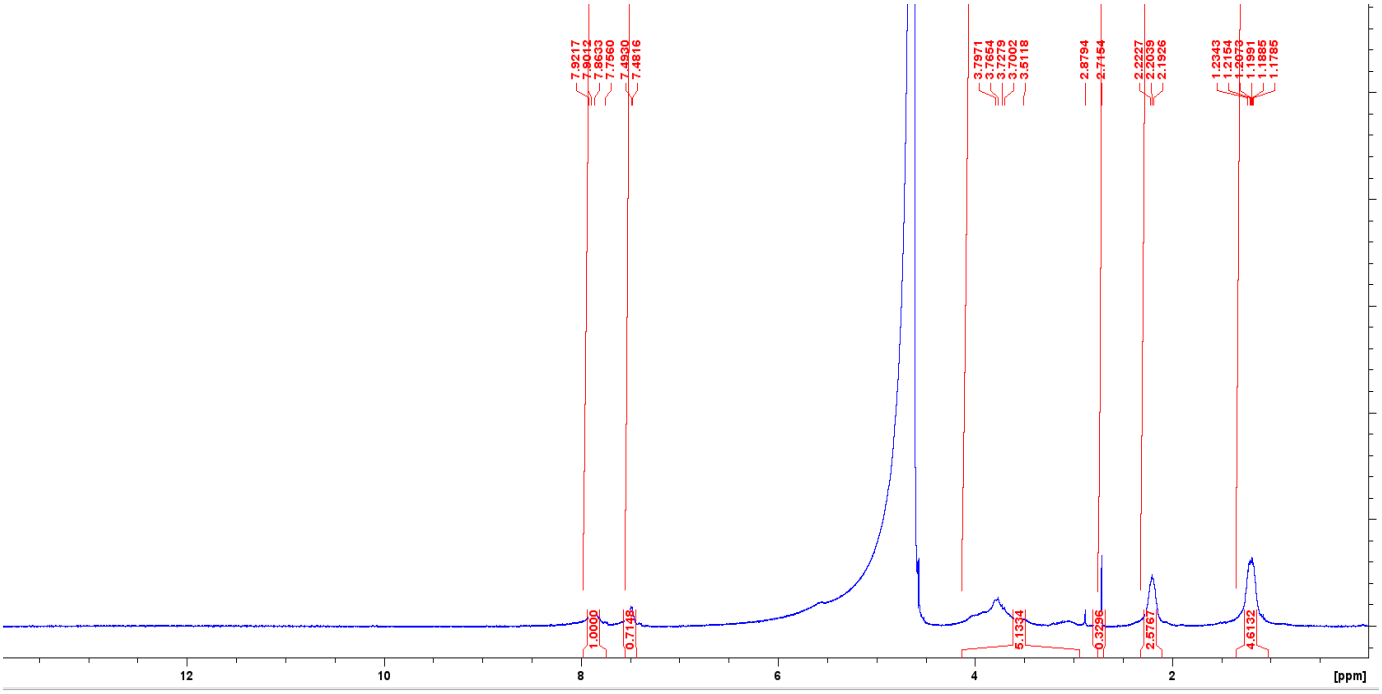

Appendix A-3. ^{1}H NMR spectrum of 2-(N-4-triethylphosphonium) benzamide chitosan run 3 (TEPBA-CS-3).

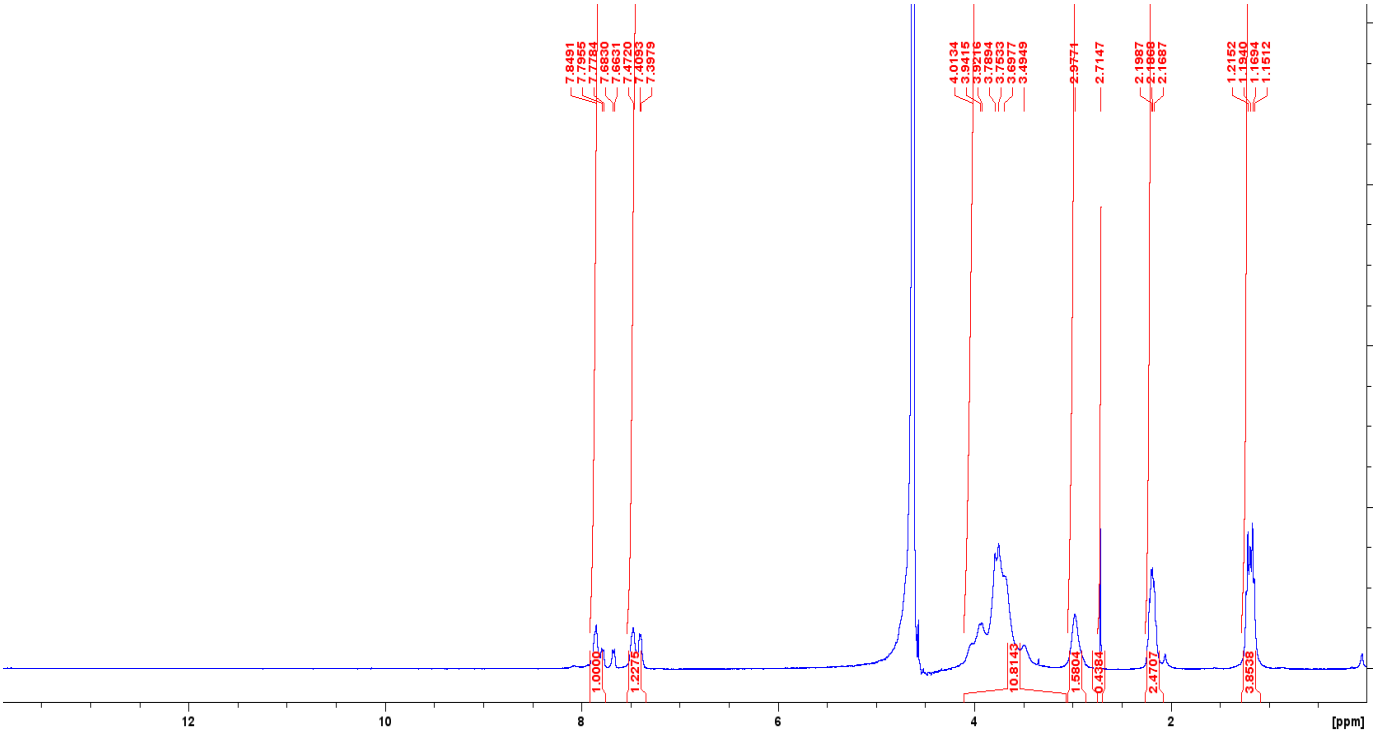

Appendix A-4. ^{1}H NMR spectrum of 2-(N-4-triethylphosphonium) benzamide chitosan run 4 (TEPBA-CS-4).

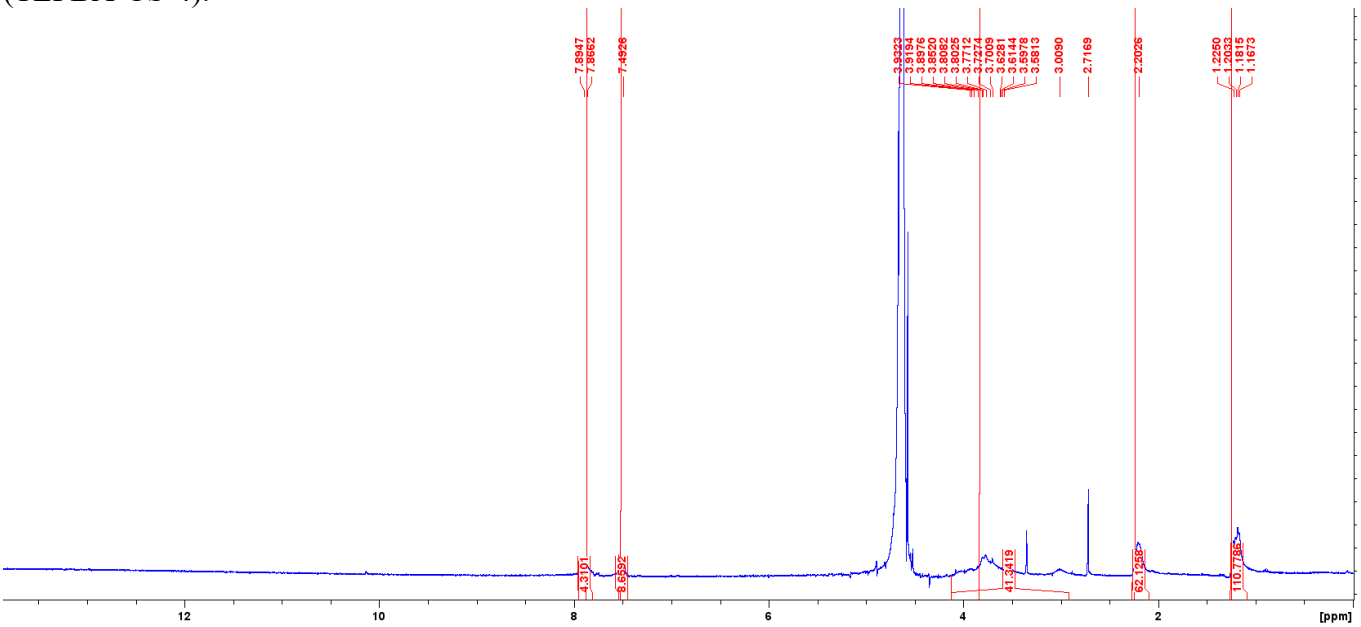

Appendix A-5. ^{1}H NMR spectrum of 2-(N-4-triethylphosphonium) benzamide chitosan run 5 (TEPBA-CS-5).

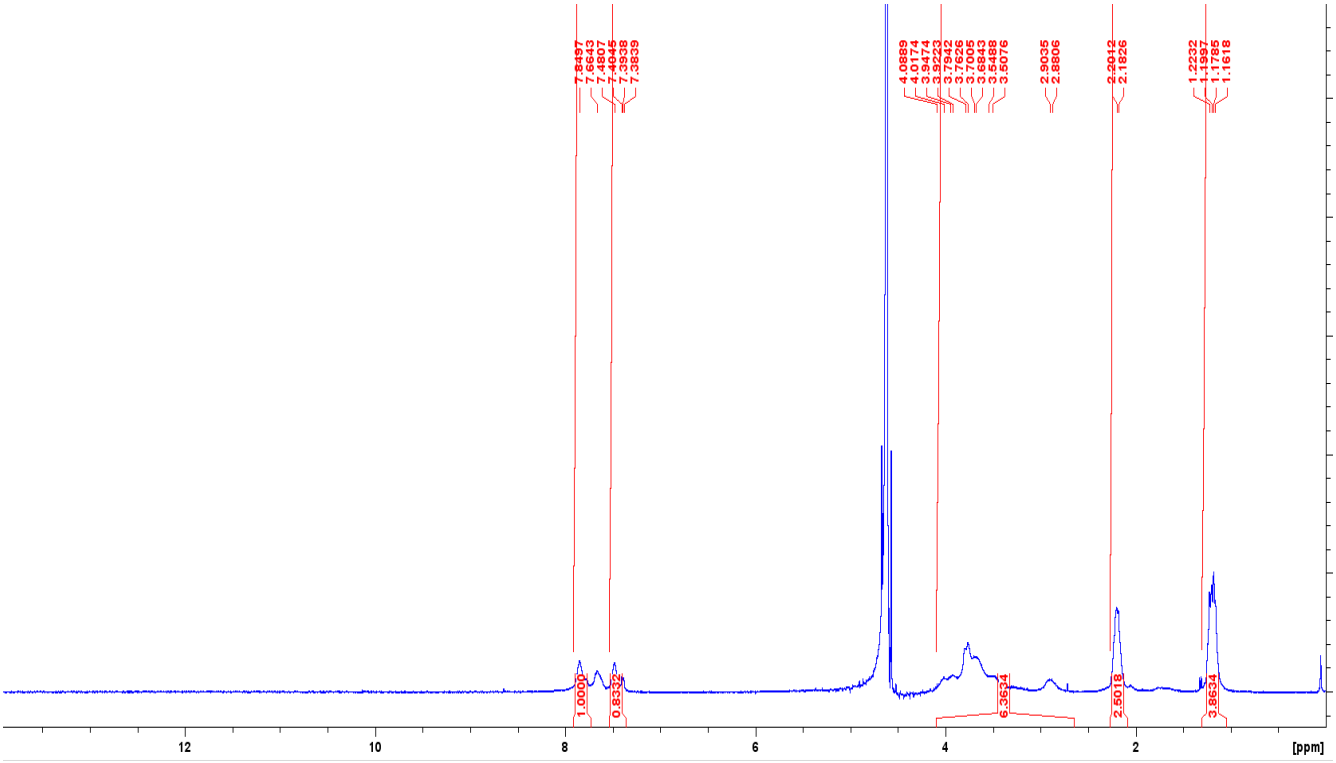

Appendix A-6. ^{1}H NMR spectrum of 2-(N-4-triethylphosphonium) benzamide chitosan run 6 (TEPBA-CS-6).

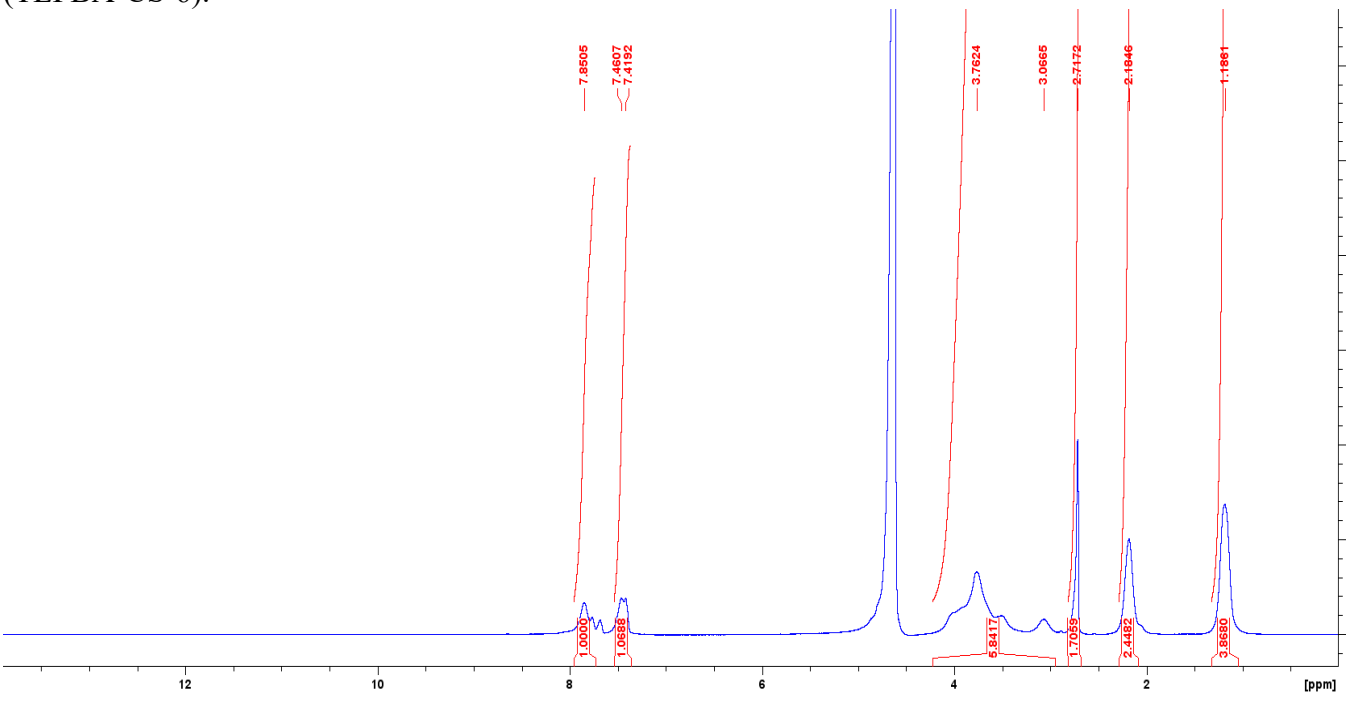

Appendix A-7. ^{1}H NMR spectrum of 2-(N-4-triethylphosphonium) benzamide chitosan run 7 (TEPBA-CS-7).

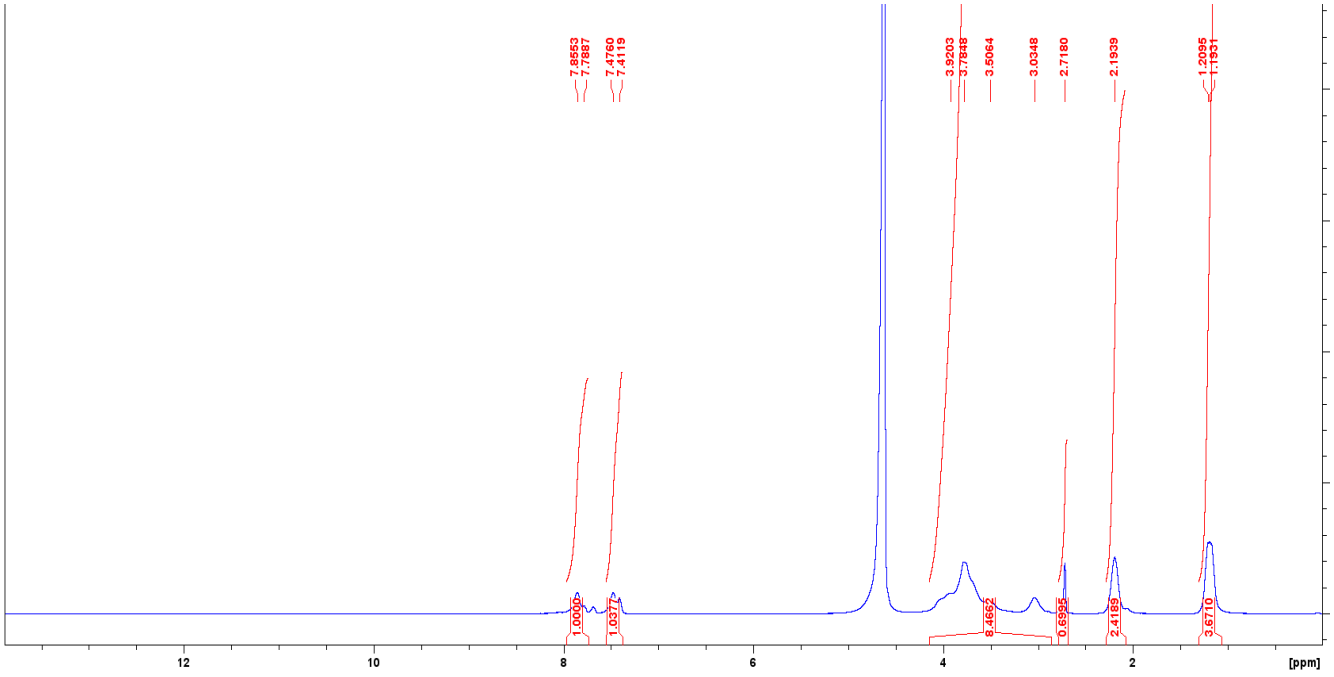

Appendix A-8. ^{1}H NMR spectrum of 2-(N-4-triethylphosphonium) benzamide chitosan run 8 (TEPBA-CS-8).

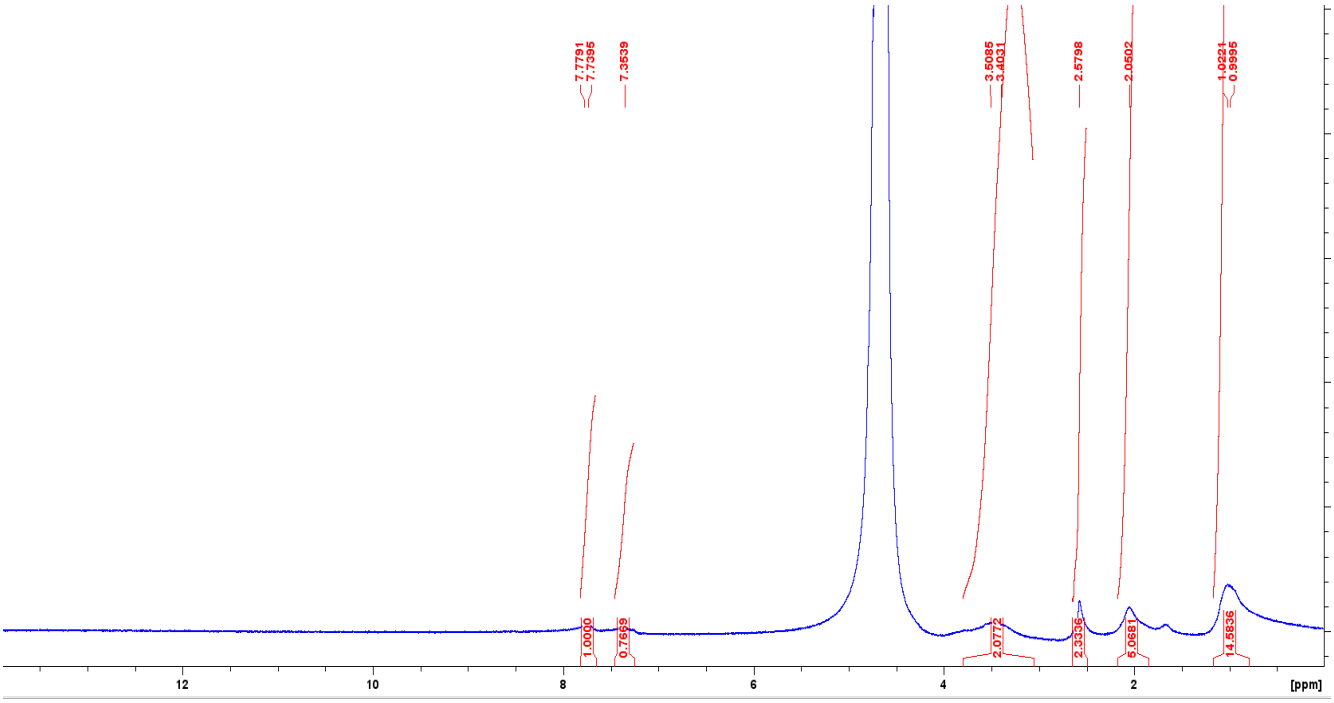

Appendix A-9. ^{1}H NMR spectrum of 2-(N-4-triethylphosphonium) benzamide chitosan run 10 (TEPBA-CS-10).

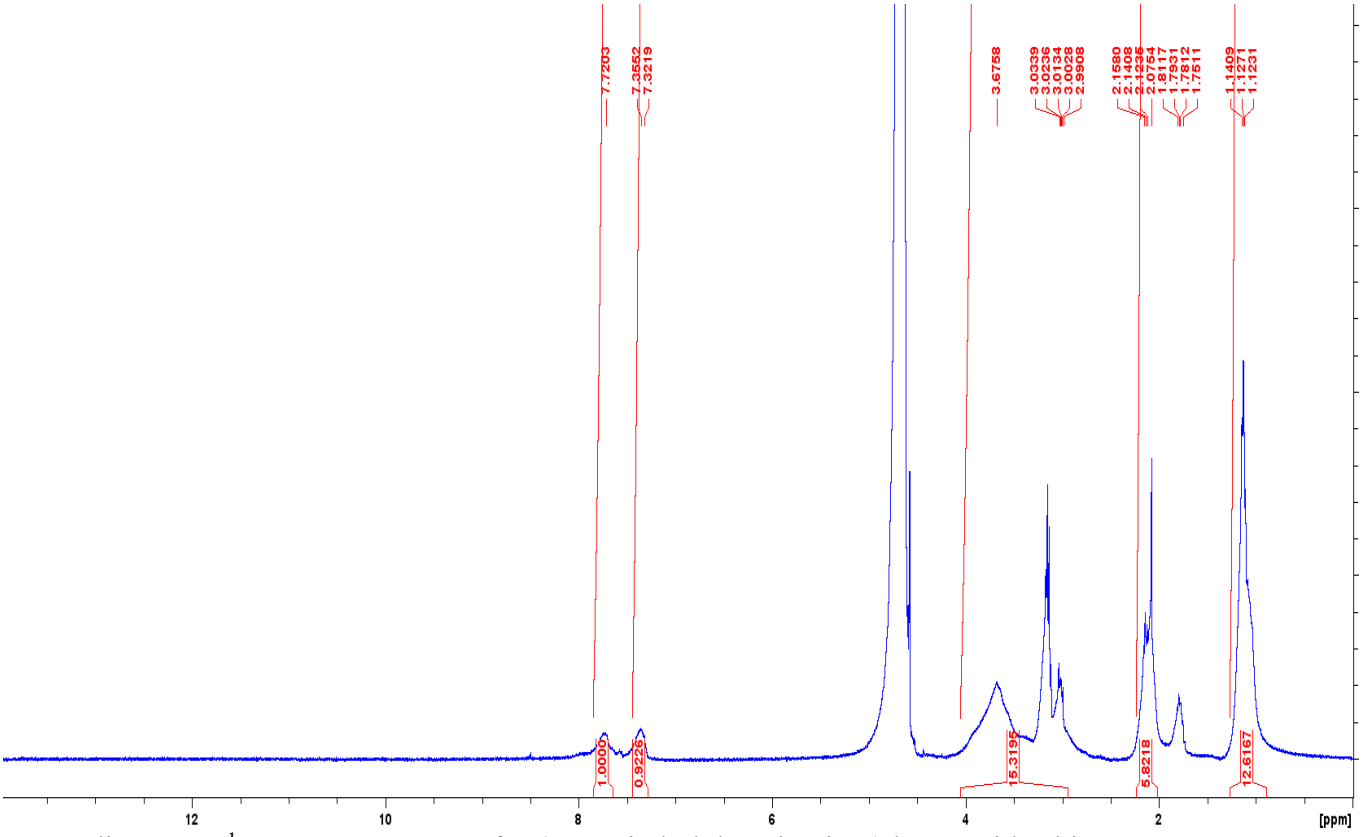

Appendix A-10. ^{1}H NMR spectrum of 2-(N-4-triethylphosphonium) benzamide chitosan run 11 (TEPBA-CS-11).

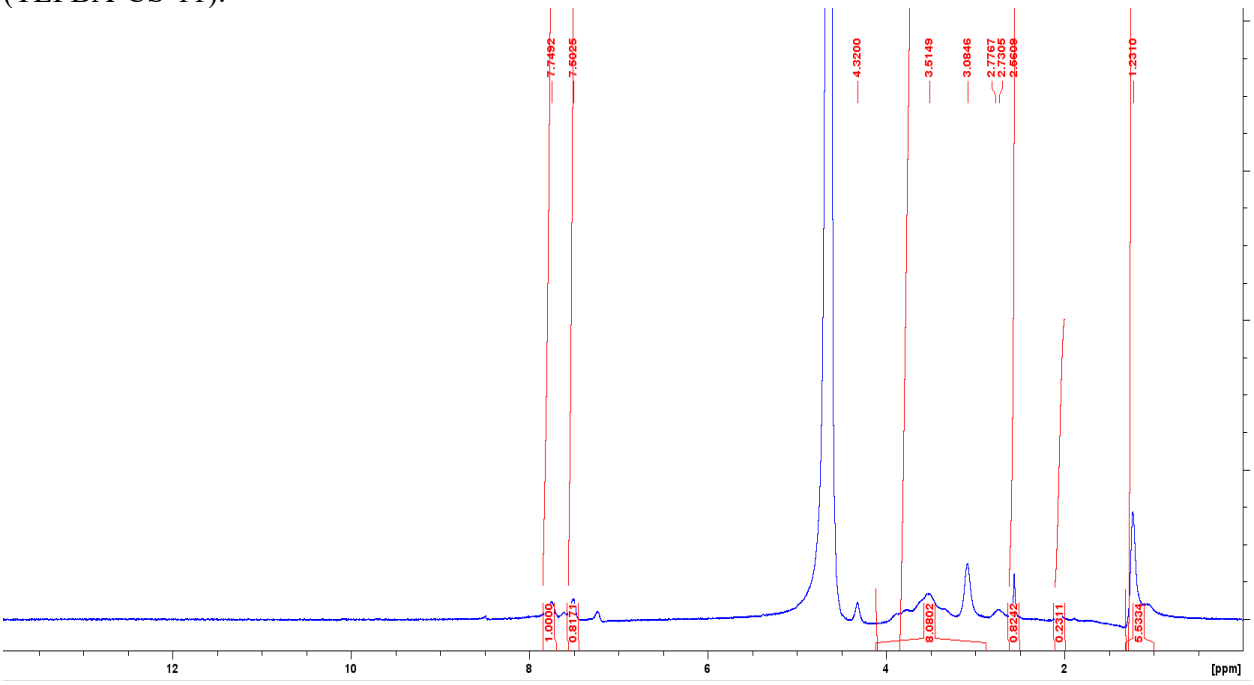

Appendix A-11. ^{1}H NMR spectrum of 2-(N-4-triethylammonium) benzamide chitosan run 1 (TEABA-CS-1).

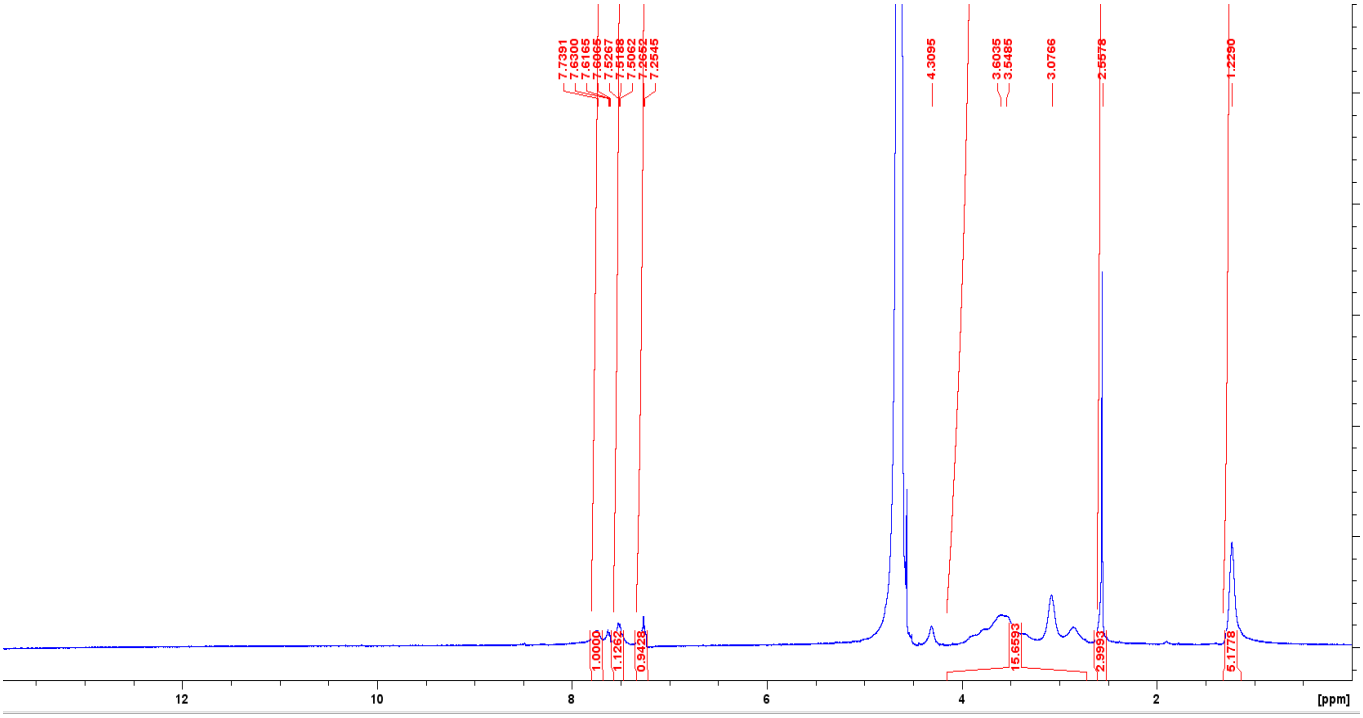

Appendix A-12. ^{1}H NMR spectrum of 2-(N-4-triethylammonium) benzamide chitosan run 2 (TEABA-CS-2).

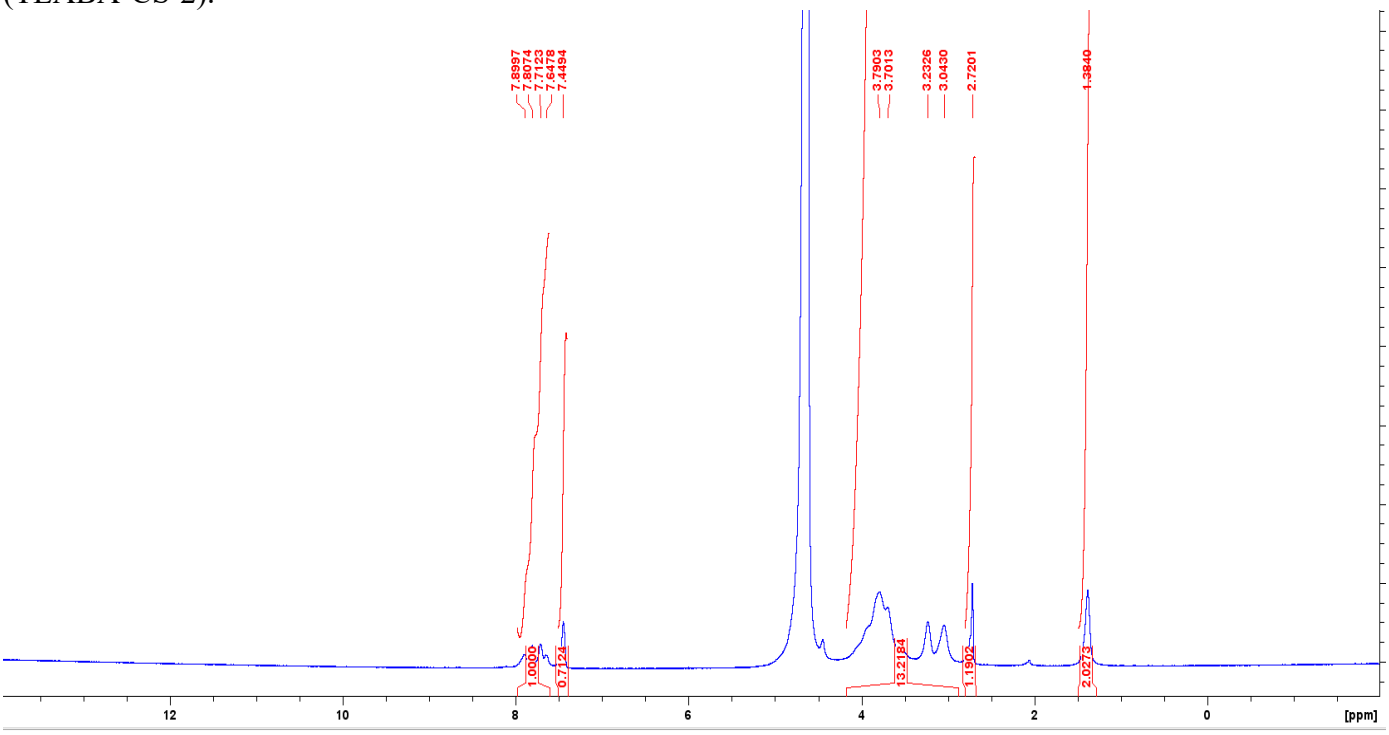

Appendix A-13. ^{1}H NMR spectrum of 2-(N-4-triethylammonium) benzamide chitosan run 4 (TEABA-CS-4).

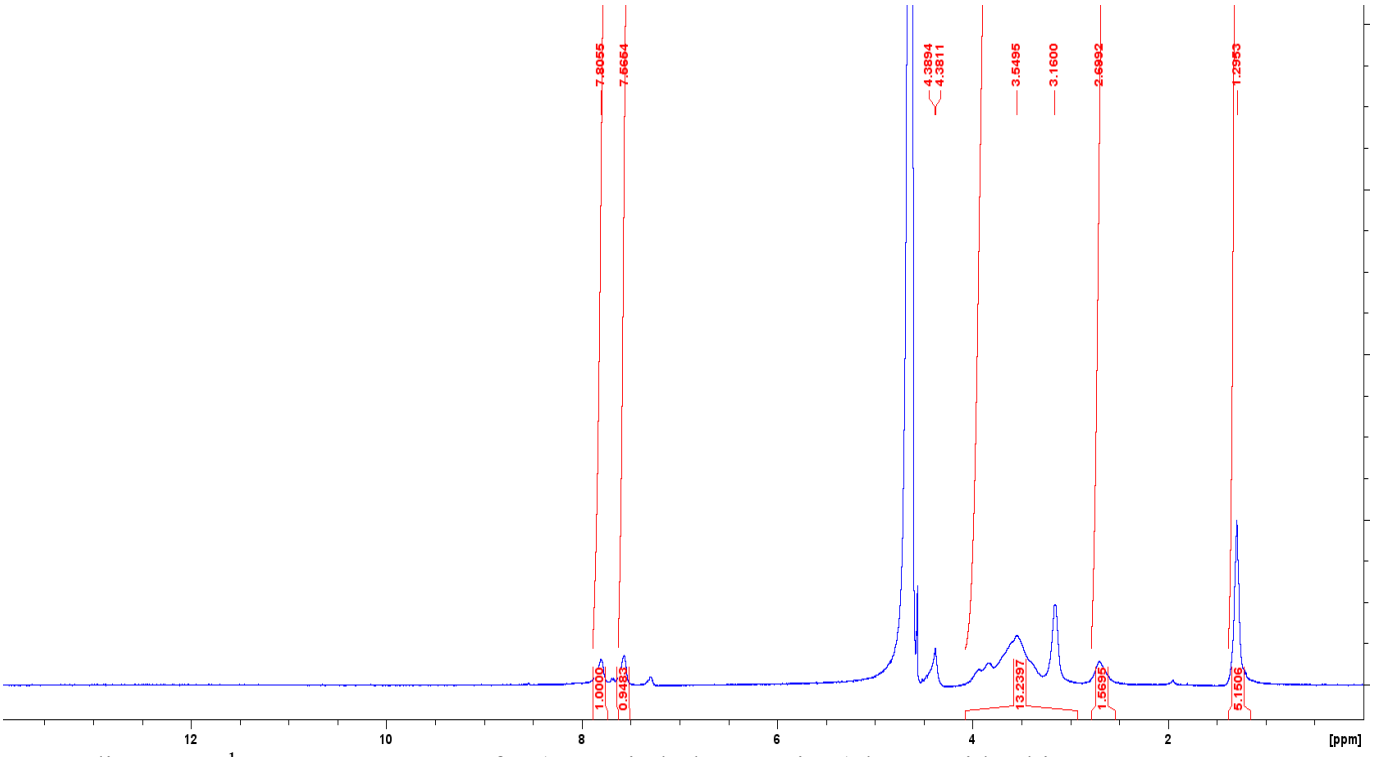

Appendix A-14. ^{1}H NMR spectrum of 2-(N-4-triethylammonium) benzamide chitosan run 5 (TEABA-CS-5).

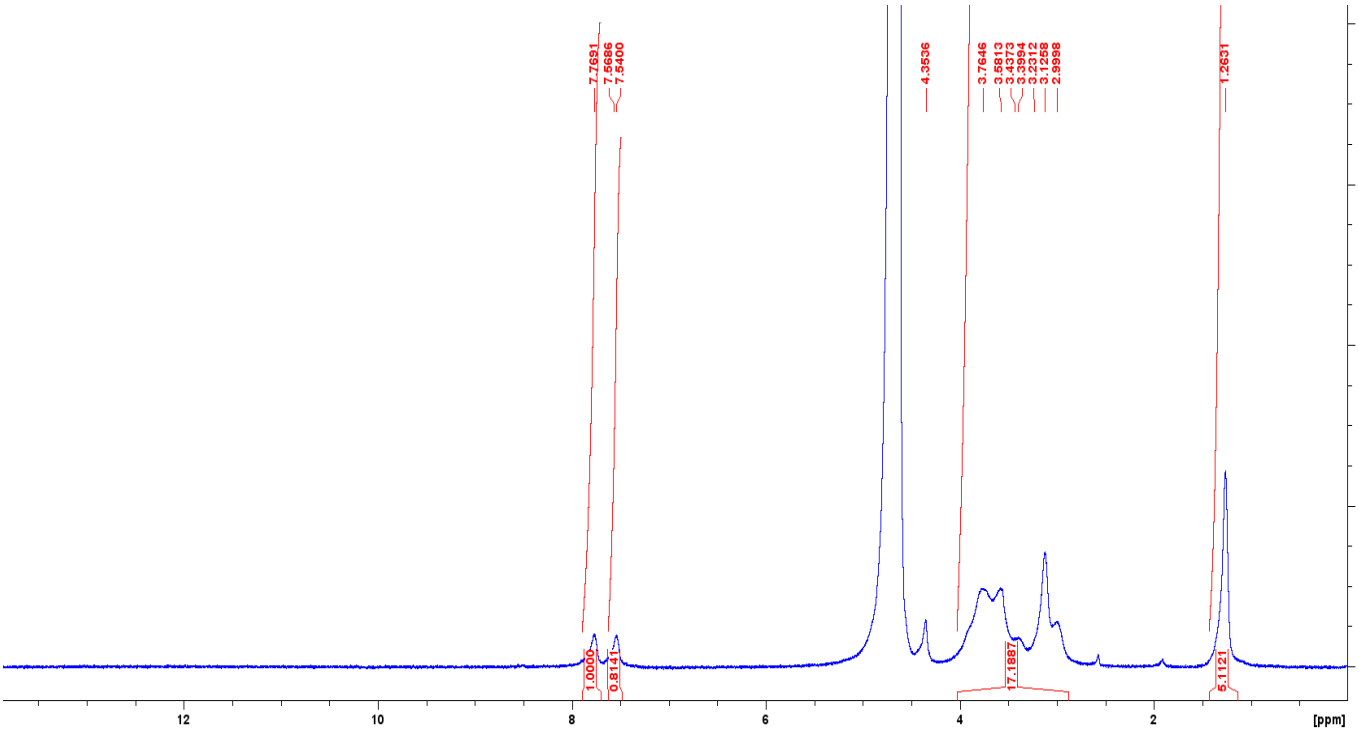

Appendix A-15. ^{1}H NMR spectrum of 2-(N-4-triethylammonium) benzamide chitosan run 6 (TEABA-CS-6).

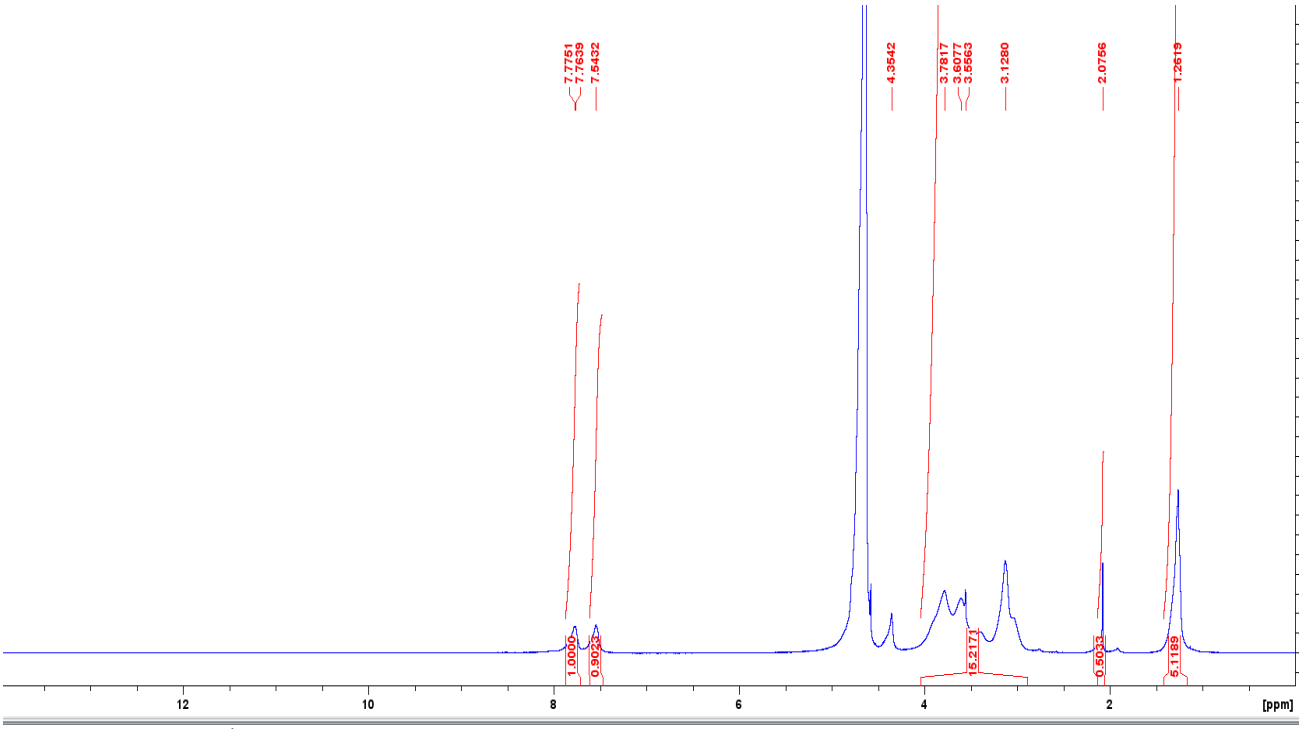

Appendix A-16. ^{1}H NMR spectrum of 2-(N-4-triethylammonium) benzamide chitosan run 7 (TEABA-CS-7).

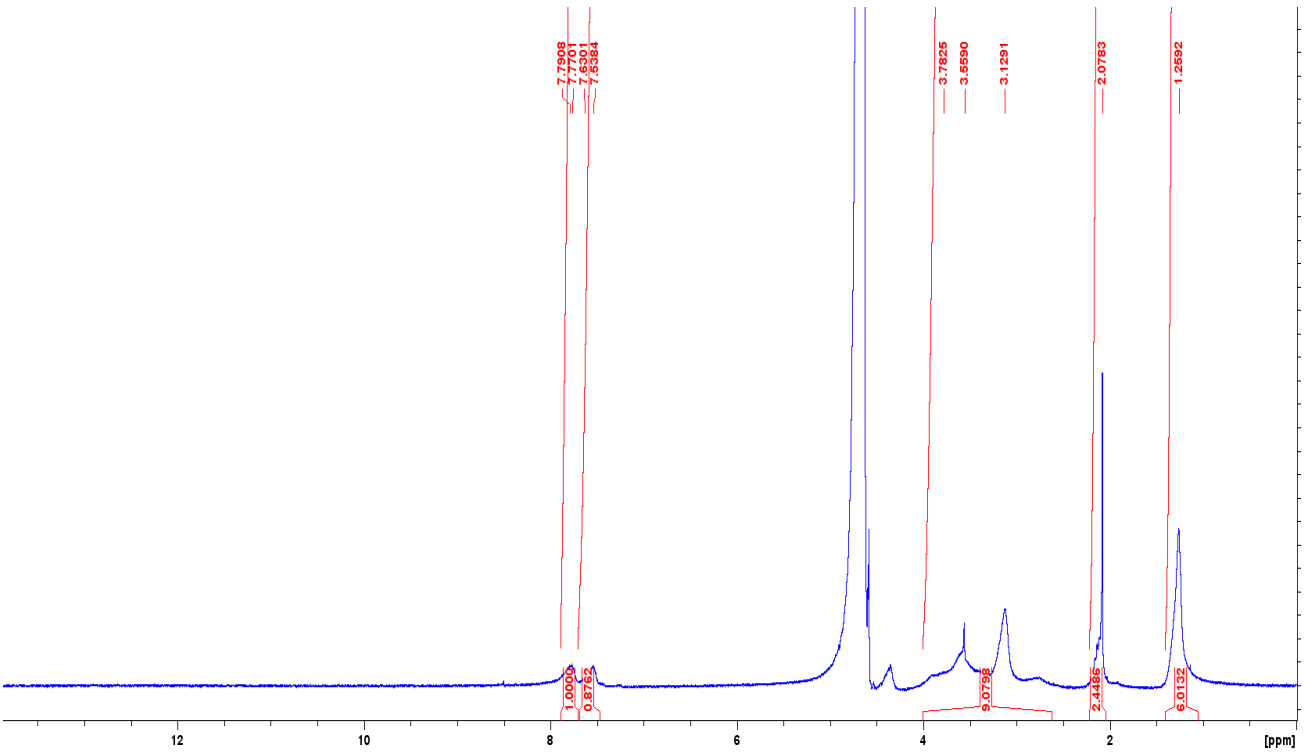

Appendix A-17. ^{1}H NMR spectrum of 2-(N-4-triethylammonium) benzamide chitosan run 8 (TEABA-CS-8).

Appendix B. FT-IR

IR spectra were collected using a Bruker Vertex 70 FT-IR spectrometer and plotted using Bruker OPUS 7.5 software. The spectra in this appendix display wavenumbers from 400-4000 cm^{-1} to display the amide, C-O, N-H, C-H, C-N^+, and C-P^+ stretch peaks found on coupled chitosan derivatives.

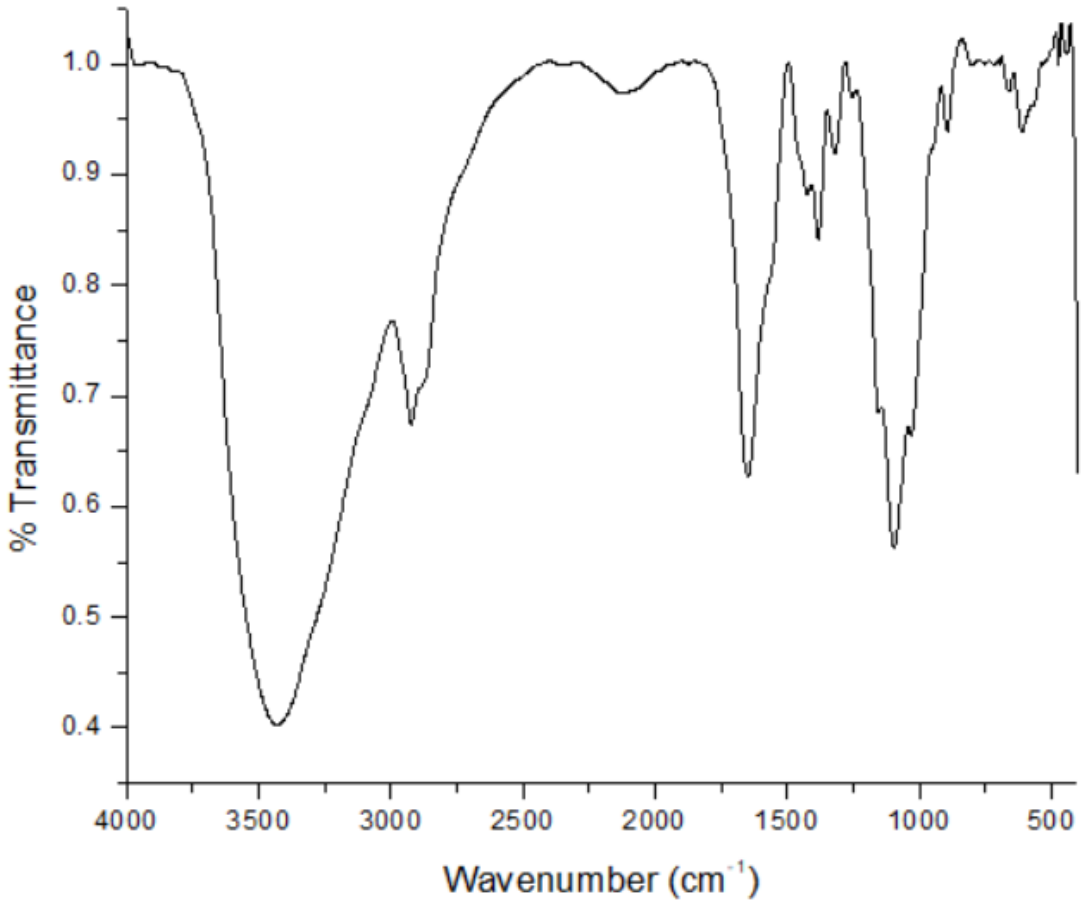

Appendix B-1. IR spectrum of 95% DA chitosan.

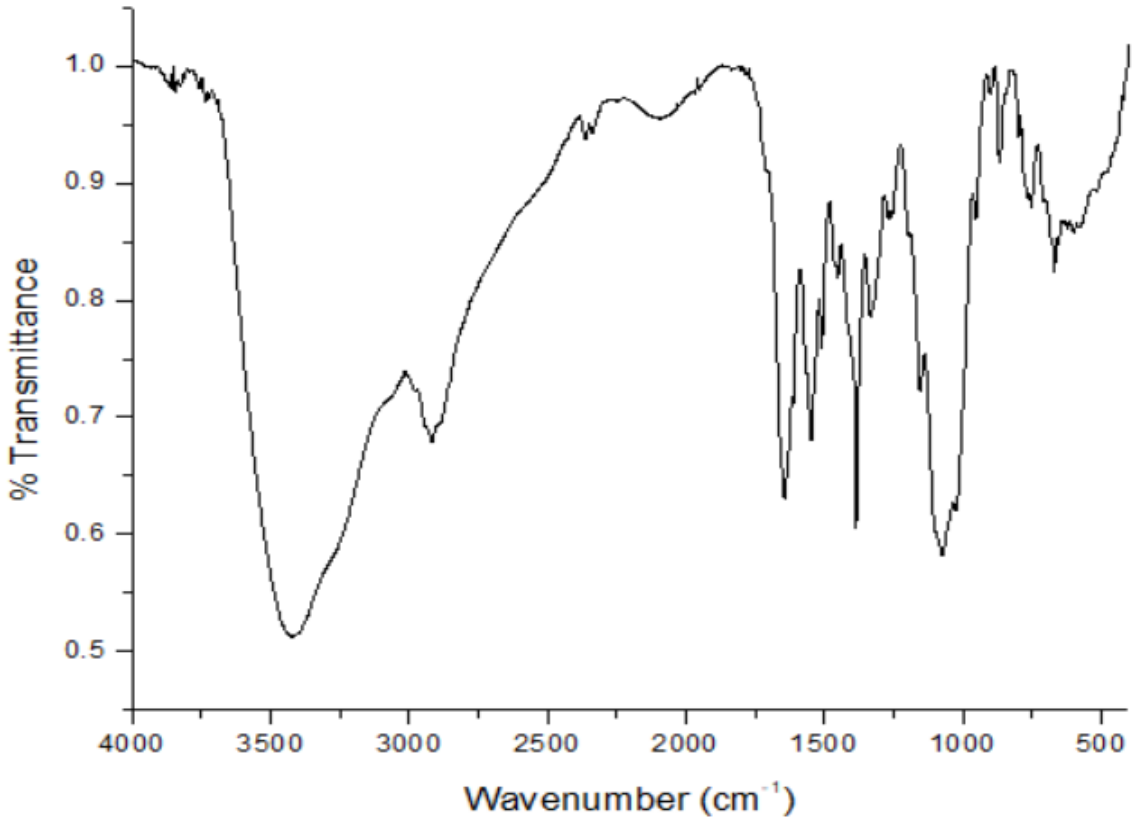

Appendix B-2. IR spectrum of 2-(N-4-triethylphosphonium) benzamide chitosan.

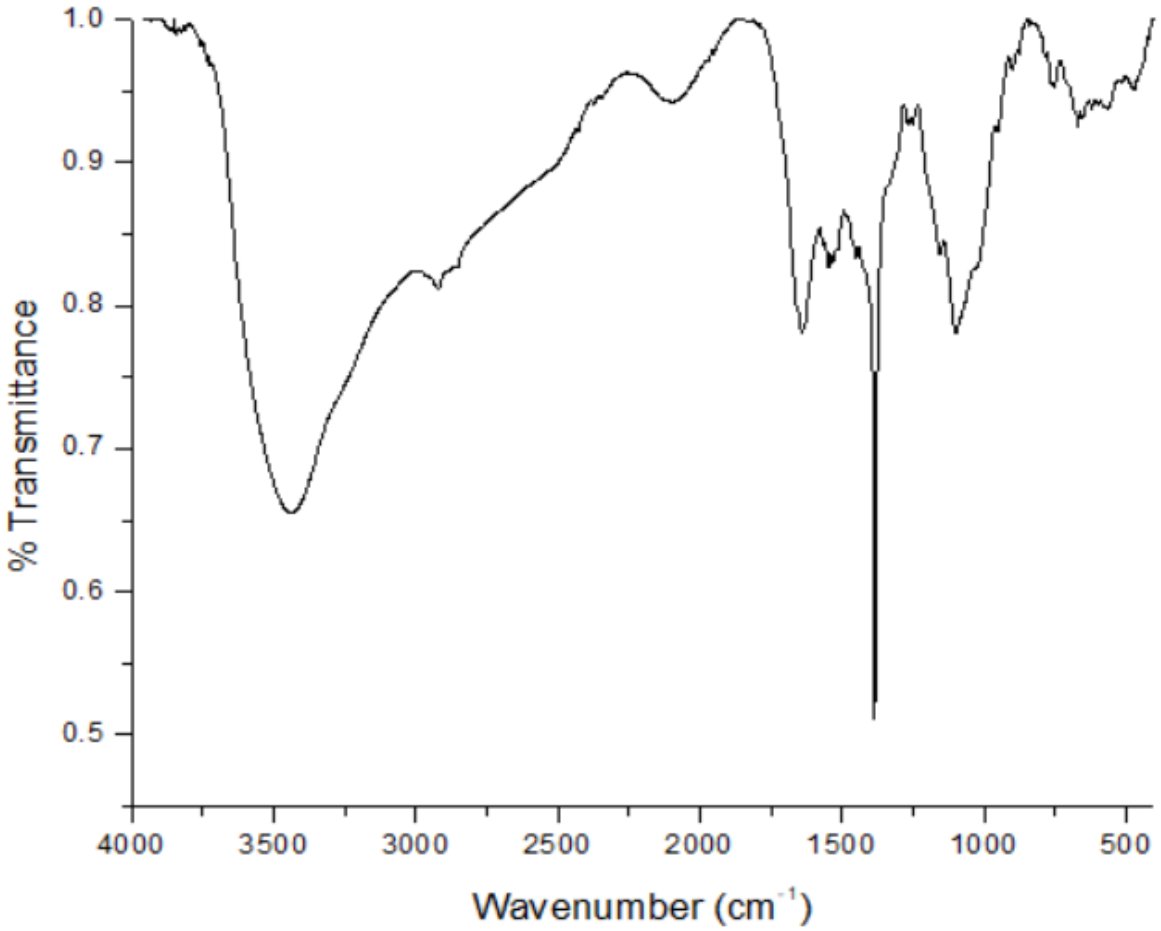

Appendix B-3. IR spectrum of 2-(N-4-triethylammonium) benzamide chitosan.